# Attachment 5

# CHLE-010:

# CHLE Tank Test Results for Blended and NEI Fiber Beds with Aluminum Addition, Revision 3

# PROJECT DOCUMENTATION COVER PAGE

| Document No: CHLE-010 | Revision: 3 | Page 1 of 50 |
|---|---|---|
| Title: CHLE Tank Test Results for Blended and NEI Fiber Beds with Aluminum Addition | | |
| Project: Corrosion/Head Loss Experiment (CHLE) Program | | Date: 2/24/2014 |
| Client: South Texas Project Nuclear Operating Company | | |

Summary/Purpose of Analysis or Calculation:

Corrosion/Head Loss Experiment (CHLE) tests are being performed to support the risk-informed resolution of GSI-191 at the South Texas Project Nuclear Operating Company (STP). This document presents the results of two multi-day tests performed in the CHLE test system (incorporating both the tank and the head loss assemblies) that evaluated methods for preparing the fiber beds for the 30-day tank tests. Two fiber preparation methods were tested: (1) fine chopping of fibers in a blender, and (2) separation of fibers using the NEI pressure-washing method.

To test the response of each fiber preparation method to the presence of chemical products, aluminum nitrate was added very slowly in successive batches over several days. The aluminum nitrate addition began after about 7 days of circulation under fiber only conditions.

| Role: | Name: | Signature: | Date: |
|---|---|---|---|
| Prepared: | Kerry Howe | < signed electronically > | 7/23/2012 |
| Reviewed: | Janet Leavitt | < signed electronically > | 8/17/2012 |
| Oversight: | Zahra Mohaghegh | < signed electronically > | 2/13/2014 |
| Approved: | Ernie Kee | < signed electronically > | 2/24/2014 |

| Revision | Date | Description |
|---|---|---|
| 1 | 7/23/2012 | Draft document for internal review |
| 2 | 8/19/2012 | Addressed internal review comments |
| 3 | 2/24/2014 | Review for NRC submittal |
| | | |
| | | |
| | | |

## Table of Contents



## List of Figures

## List of Tables

## Introduction

The purpose of this report is to describe the results from experiments conducted as part of the Corrosion Head Loss Experimental (CHLE) program. The CHLE tests are being conducted at the University of New Mexico to investigate long-term chemical effects on Emergency Core Cooling System (ECCS) strainer debris beds under prototypical conditions for the South Texas Project in support of the NRC Generic Safety Issue (GSI) 191 risk-informed resolution. Two objectives within the CHLE program are to determine (1) whether or not chemical precipitates can form in the post loss-of-coolant accident (LOCA) environment, and (2) whether any observed products either nucleate directly on or accumulate within prototypical fiberglass debris beds.

An important consideration is that the fiber debris beds that are used in the chemical effect testing be suitable surrogates for debris that would be formed during a LOCA. Attributes that affect the suitability of a particular debris bed design include the stability of the debris bed, the reproducibility of the results, and the ability of the debris bed to participate in chemical interactions under a variety of conditions. Debris beds used in some previous GSI-191 work are not necessarily applicable to the current study for three reasons. First, the approach velocities historically used in head loss testing were more than an order of magnitude higher than the STP strainer design. Second, the historical observations were typically for short periods compared to the CHLE investigations. Third, the Nuclear Energy Institute (NEI) has recently developed a debris preparation method [1] that is believed to be prototypical of debris formed during a LOCA, and most previous head loss testing have used other debris preparation methods. The Nuclear Regulatory Commission (NRC) reviewed the NEI plan and noted it is generically an acceptable way of producing debris, but declined to officially endorse it as the only way to produce acceptable debris because of the dependence on human actions [2].

Two types of fiber bed preparation methods have been evaluated for possible use within the CHLE program. First, the most recent debris formulation advocated by NEI for strainer testing involves baking fiber blankets on one side at 300 °C for 6 to 8 hours, followed by disaggregation with a commercial pressure-washer; this method is referred to as the NEI pressure-washing method in this report. Second, fiber blankets were subjected to the same backing procedure, but were separated by fine chopping of fibers in a blender. A previous report, *CHLE-008: Debris Bed Preparation and Formation Test Results* [3] performed an initial investigation of these debris bed preparation methods with respect the attributes for suitability described above. The experiments described in that report found that the NEI pressure-washing method resulted in more stable and reproducible debris beds than the blended bed method in relatively short (several hour) head loss tests. However, the blended debris beds experienced greater head loss when precipitates prepared according to the WCAP protocol were introduced directly into the head loss assemblies or into the CHLE tank, leading to the perception that the blended fiber debris beds are more sensitive detectors for the presence of precipitates.

The current test results extend the knowledge about the suitability of these debris preparation methods, and provide additional information about the formation of precipitates in the prototypical chemical environment. The tests had two key components. First, the stability and reproducibility of the debris beds were investigated over a longer period (about 7 days) to

evaluate whether the debris beds would be suitable for the long-term CHLE tests, which may be up to 30 days long. This portion of the study was conducted with no corrosion materials in the tank or corrosion products added to the solution. Second, after 7 days of fiber-only operation, aluminum nitrate was slowly injected into the tank to simulate the slow release of aluminum that would occur as the result of corrosion. This aluminum addition method is believed to be a closer surrogate for corrosion product introduction than direct addition of the WCAP formulation.

The key objective for selection of bed morphology in the CHLE program is that the debris type be representative of nominal beds that are likely to accumulate within the spectrum of break sizes; i.e., the bed should not be artificially constructed. The tests described here explore the attributes of two alternative bed preparation methods; both of which might be considered realistic under different recirculation flow regimes, but neither which can alone fully inform the resolution of chemical induced head-loss affects. Therefore, practical considerations regarding test stability for the purpose of studying 30-day chemical behavior is a dominant concern for the selection of a debris preparation protocol. Head loss through debris beds involves a wide variety of physical phenomena. These phenomena include initial debris size, fiber separation, and fiber fracture, prototypical debris transport, and accumulation. None of these factors affects the chemical behavior of fiberglass in the system, but all of these factors affect the degree of head loss that can be experienced at the strainer. Issues like particulate to fiber ratio, maximum bed thickness, thin bed formation under quiescent flow conditions, etc. will be studied systematically in the vertical head-loss test series.

The testing program was conducted from 28 June 2012 to 24 July 2012. Throughout the tests, the chemical system in the tank was prototypical of the post-LOCA chemical environment at STP; the chemicals included boric acid, trisodium phosphate, lithium hydroxide, hydrochloric acid, and nitric acid. The support screen use was prototypical of the ECCS strainers at the STP plant. A temperature profile characteristic of a medium-break LOCA as predicted by MELCOR and RELAP-5 was used. The approach velocity to the debris beds was 0.01 ft/s to be consistent with the strainers at STP.

The results of this series of tests are summarized in the next section, and detailed results of the tests are presented after that.

## Summary of Results

The following conclusions can be drawn from this test series:

- The fiber beds prepared with blending in a blender were not reproducible between columns. After 6 days of operation, the head loss varied from 1.2 inches of water to 61 inches of water through debris beds that were circulating the same water at the same rate (see Figure 1).
- The fiber beds prepared with the blended preparation method formed small, dense nodules of fiber at the base of the fiber bed, immediately adjacent to the perforated support plate. The nodules formed a dimple pattern that matched the pattern of holes in

the perforated plate, indicating that the smaller fibers formed by the blending process were able to form a more dense fiber mat in a localized area (see Figure 14).

- The difference in head loss among the three columns with the blended fiber preparation appears to be due to a trace amount of dirt or other material that collected in the small, dense fiber nodules at the base of the fiber bed. The debris bed with the highest head loss visually had the greatest amount of darker material present in the nodules. The fiber beds were visibly clean through the rest of the depth, suggesting that little or no head loss occurred through the bulk of the depth of the fiber bed and that nearly all of the head loss occurred in the fiber where it contacted the perforated plate, indicating significant nonhomogeneity to the head loss characteristics of the bed (see Figure 14).
- The fiber beds prepared with the NEI pressure-washing method were reproducible between columns. After 6 days of operation, the head loss varied from 0.36 inches of water to 0.48 inches of water through debris beds that were circulating the same water at the same rate (see Figure 2). Similar behavior continued until the test was terminated after 12 days.
- The fiber beds prepared with the NEI pressure-washing method did not form the dense nodules of fiber that were observed with the blended fiber beds (see Figure 15). The absence of these nodules and the reproducible behavior of the NEI beds lends further credibility to the conclusion that these nodules were responsible for the non-reproducible behavior of the blended fiber beds.
- The blended fiber preparation method resulted in shorter fibers (often called "shards" or "fragments") than with the NEI pressure-washing method (see Figure 9 and Table 1), which may have led to the ability of the bed to form the dense nodules at the holes in the perforated plate. The shorter fibers led to a more compact debris bed (see Figure 10). Low porosity nodules are formed by local bed compaction, enabled by the mobility of short fiber shards formed during the chopping procedure. Local compaction in regions of flow acceleration near the strainer penetrations is further enabled by loosely aggregated beds formed under very low approach velocity.
- The debris beds did not change thickness significantly over the course of the test, which lasted over 8 days for the blended fiber debris bed and over 12 days for the NEI fiber debris bed (see Figures 11 and 12). Further, minimal differences in thickness were observed between beds despite the wide variation in measured pressure loss. The lack of change in bed thickness, coupled with the visually clean nature of the debris beds, lends credibility to the conclusion that the head loss associated with the blended fiber debris bed was due to localized conditions at the perforated plate.
- Turbidity was an excellent indicator of the precipitation of aluminum hydroxide precipitates in solution (see Figure 22, 23, and 24).
- Essentially all of the aluminum that was added to solution formed a precipitate, as indicated by turbidity measurement and supported by total and filtered aluminum analyses.
- The addition of 1 mg/L of aluminum in solution caused the formation of in-situ precipitates that caused head loss through the blended fiber debris beds. An additional 5 mg/L (6 mg/L total) caused sufficient head loss to terminate the test (see Figure 29).
- Aluminum in solution in the form of pre-formed WCAP precipitates also caused head loss sufficient to terminate a similar blended fiber debris bed test (see Figure 30).

- The addition of up to 40 mg/L of aluminum over a period of 6 days was not sufficient to cause head loss through the NEI fiber debris beds (see Figure 31). However, the same amount of aluminum in the form of pre-formed WCAP precipitates caused extensive head loss that terminated a similar test within 3 hours (see Figure 32). These results indicate that precipitates formed in-situ through the addition of aluminum nitrate at a slow rate have significantly different characteristics from those of the pre-formed WCAP precipitates.
- Particle size analyses indicate that the size of precipitates formed in-situ are up to 10 times smaller than the pre-formed WCAP precipitates with similar solution conditions (0.17 μm versus 1.6 μm in diameter, see Table 2). This significant difference in size appears to be sufficient to cause the pre-formed WCAP precipitates to be retained by the NEI fiber debris beds but allow the in-situ precipitates to pass through the NEI fiber debris beds. The results indicate that head loss may be less significant than indicated by the use of pre-formed WCAP precipitates, depending on the filtration characteristics of the debris bed.
- Zeta potential analyses indicate that solution chemistry affects the surface charge of pre-formed WCAP precipitates. When tests were conducted in deionized water, pre-formed WCAP precipitates had a positive zeta potential. When tests were conducted in Albuquerque tap water, the pre-formed WCAP precipitates were nearly neutral. When tests were conducted in water containing boric acid and TSP, the precipitates had a significant negative charge. The reversal of charge depending on solution chemistry suggests that head loss testing using pre-formed WCAP precipitates may not adequately predict the extent of head loss through a strainer under conditions in which debris beds are not reliant on physical sieving for the retention of particles.
- Despite the slow introduction of aluminum nitrate, corrosion conditions were not perfectly emulated. It is possible that conditions that minimize aluminum release, such as the passivation of aluminum surfaces or the formation of a low-solubility oxide layer, would result in an upper limit to the aluminum concentration measured in solution. In addition, saturation conditions relevant for direct nucleation of precipitation products within the fiber bed may have been artificially exceeded. If direct nucleation is a credible formation mechanism, then the tests reported here best describe the filtration behavior between the two preparation methods and not necessarily the in-situ head-loss sensitivity. Direct nucleation would avoid the complications of particle filtration, perhaps leading to different head loss response in the debris beds. As a result, additional tests that investigate precipitate formation under prototypical corrosion conditions are needed.

The following sections of this report provide detailed results from the experiments. Individual sections are presented on (1) head loss, (2) approach velocity, (3) temperature, (4) bed formation and morphology, (5) water chemistry, and (6) effect of aluminum addition. Following those sections, overall conclusions of this test series are presented.

## Head Loss through Fiberglass Debris Beds

The primary diagnostic parameter monitored during these tests was the head loss through the fiberglass debris beds. The head loss through the two types of debris beds differed from each other as displayed in Figures 1 and 2. For the blender-chopped bed, the head losses through the

three beds were relatively similar to each other during the initial period of operation. The head losses through beds 1, 2, and 3 were 0.6, 0.6, and 0.9 inches of water column after 90 minutes of operation, respectively, and 0.6, 0.6, and 1.0 inches of water after 5 hours of operation, respectively. As time progressed, the head losses through the beds deviated more. After 1 day of operation, the head losses through beds 1, 2, and 3 were 0.7, 1.4, and 6.2 inches of water, respectively. After 6 days of operation, the head losses through beds 1, 2, and 3 had stabilized at 1.2, 21, and 61 inches of water, respectively, a 50-fold difference between beds 1 and 3.

Head loss depends on characteristics of the debris bed and the fluid passing through the bed. Changing water temperature causes changes in fluid viscosity and density that changes the measured head loss. To isolate changes in head loss due to changes in bed morphology independently of the changes in fluid viscosity and density, the head loss data can be corrected to a constant temperature. The head loss data was corrected for viscosity by applying the ratio of water viscosity at the measured and standard temperatures, and corrected for density by calculating the change in static head between pressure taps due to the decreasing fluid density at higher temperature. In Figures 1 and 2, the head loss data have been corrected to a temperature of 104 °F (40 °C), which is the approximate temperature at the end of each of the tests.

The debris beds prepared with the NEI pressure-washing protocol were more consistent with one another and more consistent over time. Column 3 started with less head loss than did the other columns, but after less than 1 day of operation, the head loss of column 3 had increased to be similar to that of the other columns. After 5 hours of operation, the head losses through beds 1, 2, and 3 were 0.64, 1.0, and 0.41 inches, respectively. After 6 days of operation, the head losses through beds 1, 2, and 3 were 0.42, 0.36, and 0.48 inches, respectively. The similar behavior between columns continued until the test was terminated after 12 days.

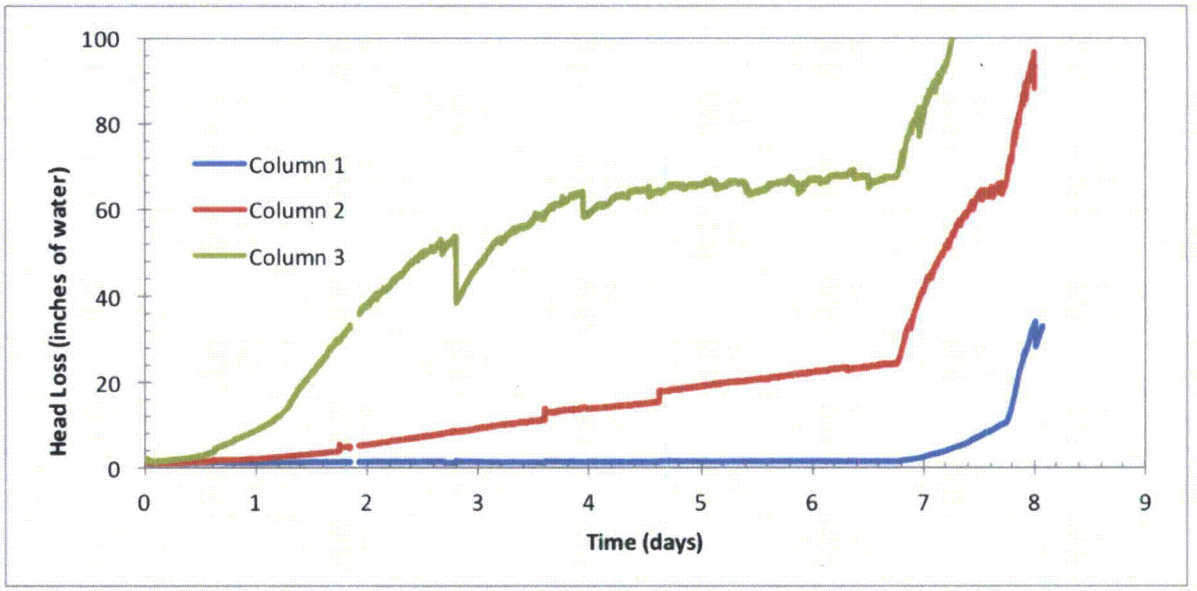


**Figure 1: Temperature-corrected head loss through fiberglass debris beds prepared by chopping in a blender (corrected to 104 °F). Aluminum nitrate addition started at about 6.75 days.**

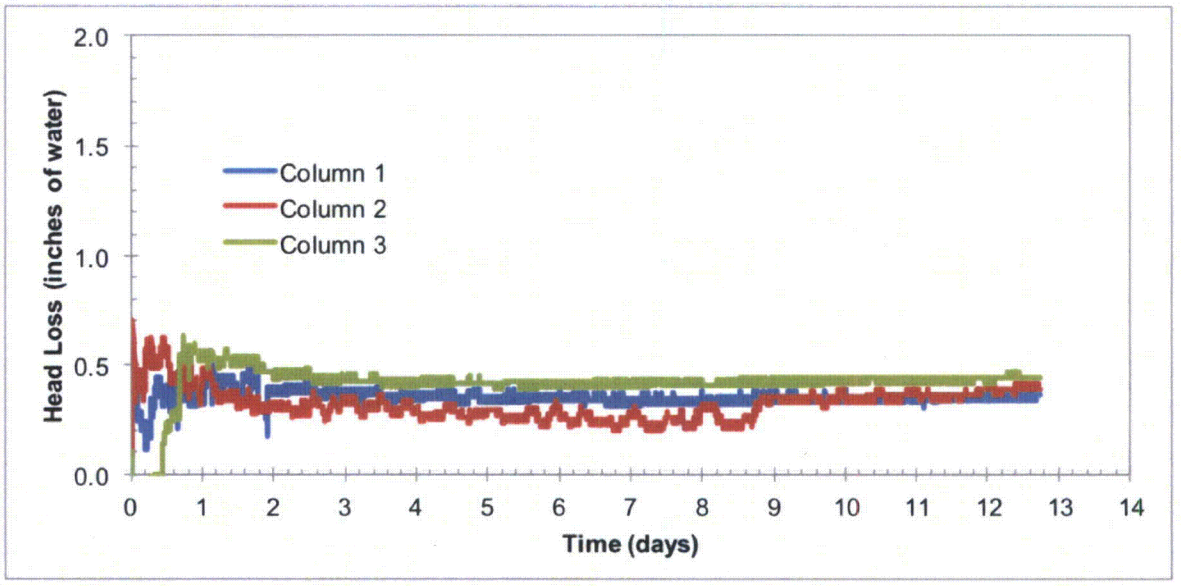


**Figure 2: Temperature-corrected head loss through fiberglass debris beds prepared using the NEI pressure-washing method (corrected to 104 °F).**

## Approach Velocity through Fiberglass Debris Beds

The approach velocity was maintained near 0.01 ft/s in all three columns for both tests. Approach velocity was adjusted by throttling a valve on the discharge side of centrifugal pumps that fed each column independently of the others. The approach velocities are displayed in Figures 3 and 4. The throttle valves required occasional adjustment to maintain the desired 0.01 ft/s approach velocity during the first several days of each test, but little or no adjustment was required later in the tests. Overall, Figures 3 and 4 show that the velocity through the debris beds was maintained at acceptable velocities over the duration of each test.

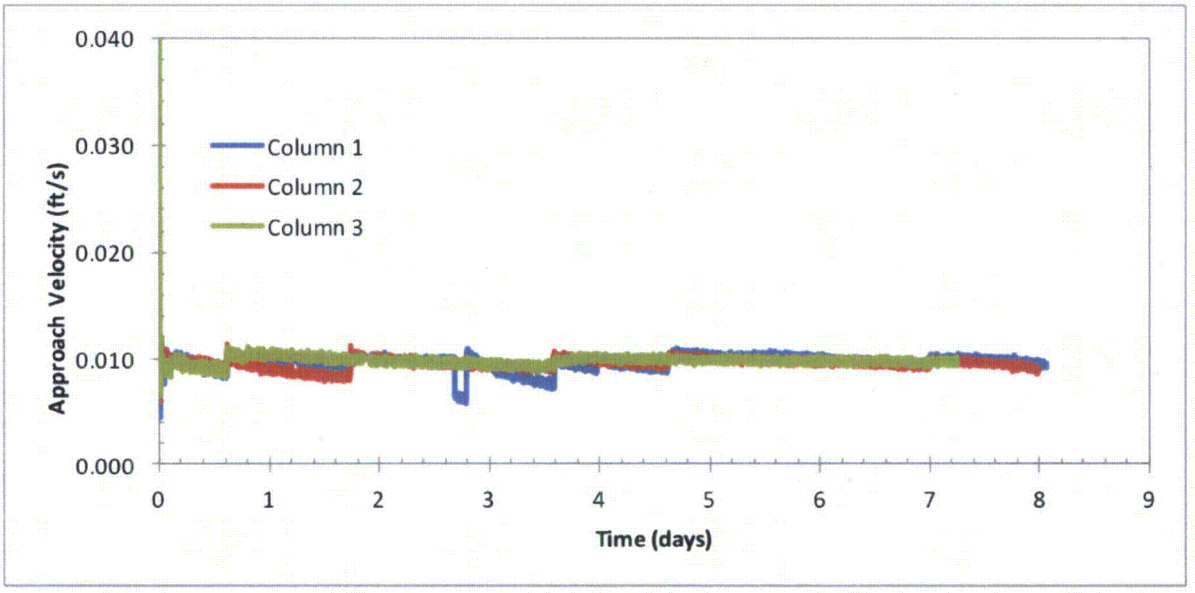


**Figure 3: Superficial filtration velocity through fiberglass debris beds prepared using the blending method.**

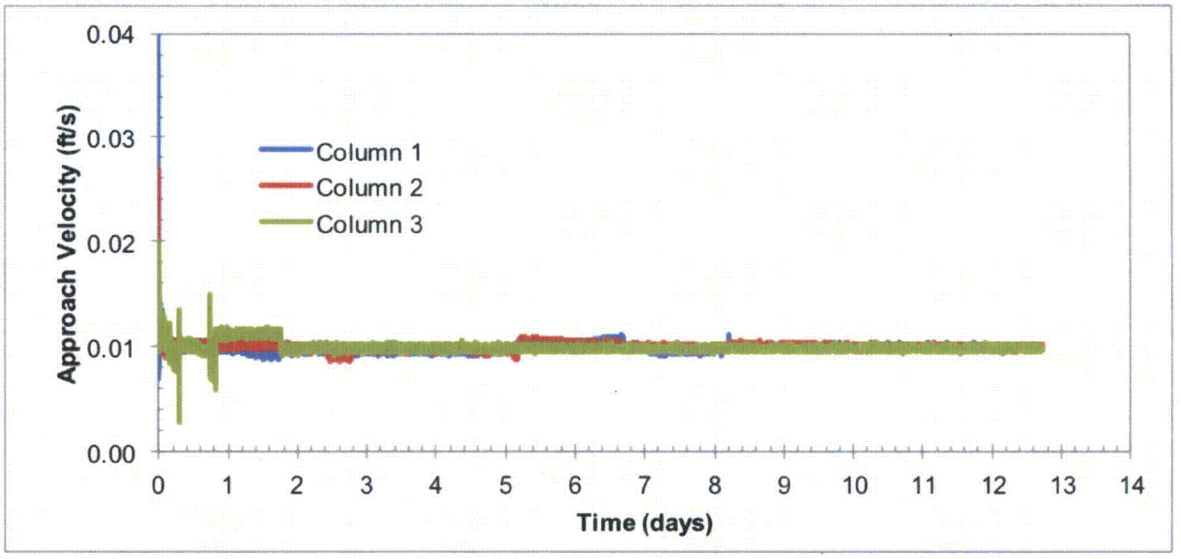


**Figure 4: Superficial filtration velocity through fiberglass debris beds prepared using the NEI pressure-washing method**

# Temperature

## Temperature Profile over Time

The temperature during each test was designed to decline over time to reflect the temperature present in the containment building following a LOCA. The temperature in these tests was modeled to emulate a break of a 6-inch pipe in containment at STP (a medium break LOCA). The target temperature profile was generated by running the MELCOR/RELAP-5 computer simulations at Texas A&M University. The predicted temperature started at about 185 °F (85 °C) and declined rapidly in the first few minutes as the leaked water came in contact with concrete and other surfaces. The temperature then increased over several hours as materials within the containment building heated up, reaching a temperature of 162 °F (72 °C) about 4 hours into the event. The CHLE temperature control system was designed to provide a more gradual decline to this temperature after 4 hours, and then to track the temperature predicted by MELCOR/RELAP-5 for the remainder of the experiment. The temperature profiles are shown in Figures 5 and 6.

During the test with the fiber beds prepared by the blending method, the temperature dropped rapidly to 162 °F (72 °C) after 4 hours into the test, but was followed by a period of constant temperature because of the failure of a temperature controller to initialize overnight. The temperature was reduced to be in compliance with the desired temperature profile before the end of the first day, and remained within 5 °F (2.8 °C) of the desired temperature until the final day of the test. The measured temperature exhibited a sawtooth pattern because the temperature controller tended to overshoot the target temperature. The increase in temperature ranged from 1.3 to 1.6 °F (0.7 to 0.9 °C) between a low-temperature reading and the next high-temperature point. Toward the end of the test, an attempt was made to adjust the deadband on the temperature controller, but the amount of overshooting increased slightly.

The operation of the temperature controller was improved for the test with the NEI pressure-washed fiber, as presented in Figure 6. The measured temperature was consistently within about 1.8 °F (1 °C) of the target temperature throughout the duration of the test and without the overshooting of the controller that had been exhibited in the test with the blended fiber.

## Temperature Variation in Tank

The temperature was measured at four locations within the CHLE tank: three in the pool and one in the vapor space. The three locations in the pool consisted of a point near the center and two points in corners of the tank. The average temperature in corners was within 0.2 °F (0.1 °C) of the temperature in the center of the tank, indicating that the thermal conditions within the tank were uniform. The comparison between the temperature in the vapor space and in the center of the pool is shown in Figure 7. In general, the temperature in the vapor space was 4 to 5 °F (2.2 to 2.8 °C) lower than the temperature in the center of the pool.

## Temperature Differential in Head Loss Columns

The temperature was also measured continuously in each head loss column about 6 inches above the debris screen. Initially, the temperature in the columns was somewhat lower than the

temperature in the tank because of heat loss in the connecting piping and in the columns. The difference in temperature between the center of the tank and column 1 is shown in Figure 8. The other columns are not shown because their results are virtually identical to column 1. At the beginning of the test, the temperature in the columns was about 1.8 °F (1 °C) lower than in the tank. But as the tank temperature decreased, the temperature difference between the tank and columns decreased. After 6 days, when the temperature in the tank had dropped to about 113 °F (45 °C), the temperature in the columns had converged to that in the tank.

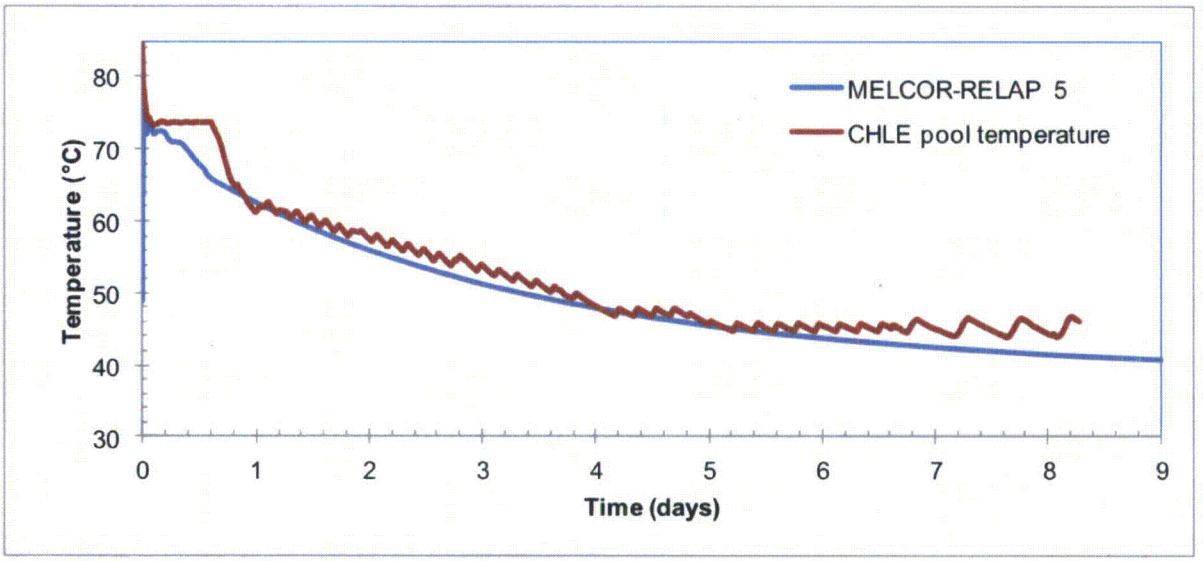


**Figure 5: Tank temperature during the experiment using fiberglass debris beds prepared using the blending method.**

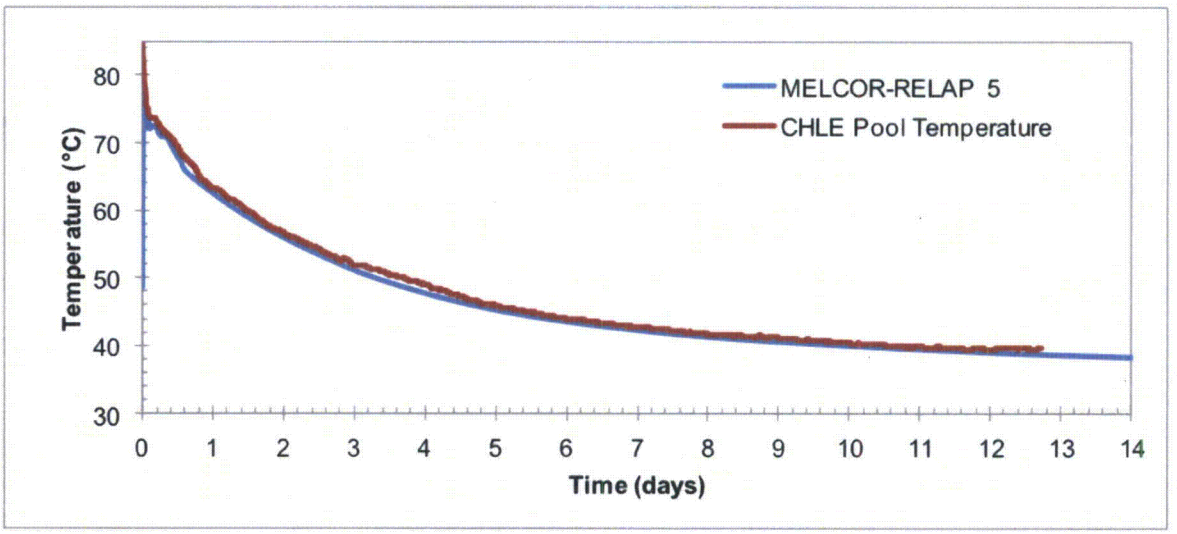


**Figure 6: Tank temperature during the experiment using fiberglass debris beds prepared using the NEI pressure-washing method.**

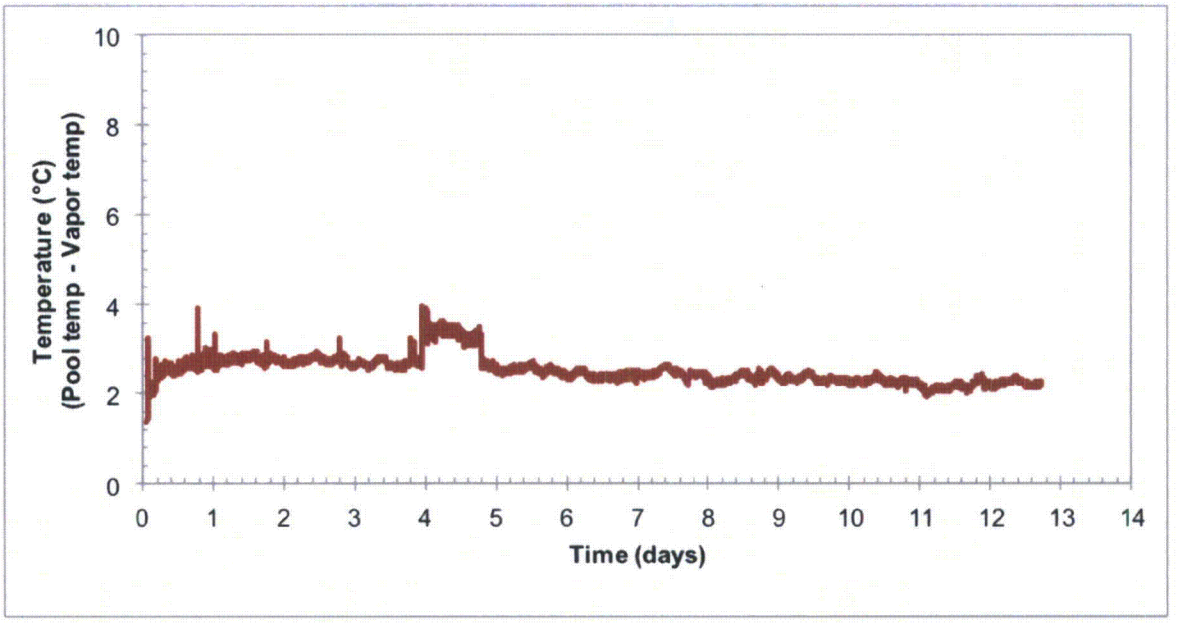


**Figure 7: Difference between the pool temperature and the vapor-space temperature in the tank during the experiment using fiberglass debris beds prepared using the NEI pressure-washing method.**

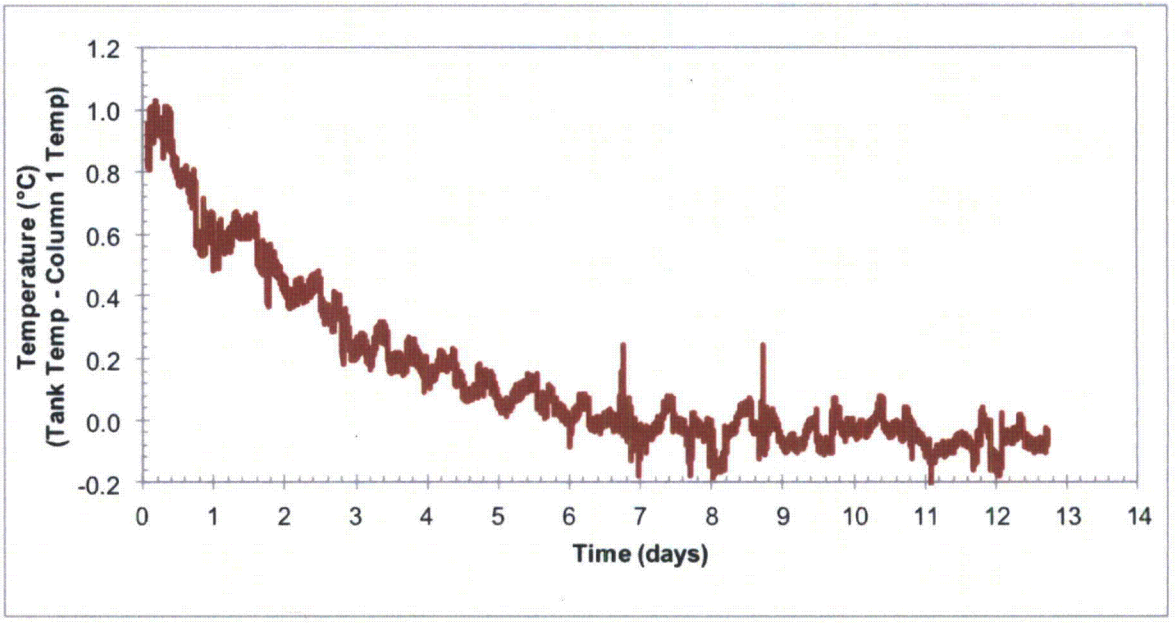


**Figure 8: Difference between the pool temperature and the temperature in Column 1 just above the debris bed during the experiment using fiberglass debris beds prepared using the NEI pressure-washing method.**

## Bed Formation and Morphology

The difference in fiber preparation resulted in variability in the characteristics of the fibers and how they formed debris beds. The difference in fiber preparation was evident when the debris was examined on a light table, as shown in Figure 9. The photographs in Figure 9 show the

contents of a 8 x 13 inch glass pan. The blended fiber preparation consisted almost entirely of individual fibers with few or no clumps. The NEI fiber preparation contained more loose clumps of fibers. In addition, the blended fiber method resulted in visually shorter fiber lengths. The visual difference in fiber length was corroborated with data on fiber length generated by IPS Testing Services, a company that measures fiber length for the paper industry [4]. IPS tested samples of fiber prepared by the two methods and reported the data in Table 1. Sixty-two percent of the blended fibers were less than 0.5 mm, but only 44% of the NEI fibers were. The measurement system could not detect the length of fibers that were less than 0.2 mm, which included 21 percent of the blended fibers and 13 percent of the fibers from the NEI preparation. IPS reported NEI fibers up to 7 mm in length, but only a maximum of 3 mm for the blended fibers.

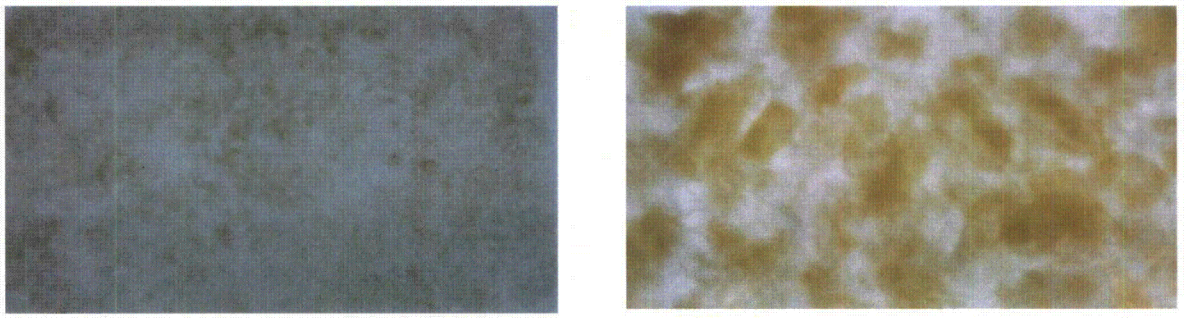

A B

**Figure 9: Examination of debris on a light table from (A) blended fiber preparation, and (B) NEI pressure-washed fiber preparation.**

Table 1: **Fiber Length of the Debris Prepared by Blended and NEI Preparation Methods**

| | Blended preparation (% of fibers) | NEI pressure-washed preparation (% of fibers) |
|---|---|---|
| < 0.5 mm | 62 | 44 |
| 0.51 to 1.0 mm | 18 | 24 |
| > 1.0 mm | 13 | 32 |

The difference in fiber preparation was also evident when the debris was placed in the head loss columns, as shown in Figure 10. The beds were formed with the same approach velocity in both tests, 0.1 ft/s. The blended fiber preparation shown in Figure 10A had an initial bed thickness of about 0.6 inches (1.5 cm), but the NEI pressure-washed fiber preparation shown in Figure 10B had an initial overall bed thickness of about 2.6 inches (6.5 cm), even though both types of fiber beds contained the same amount of fiber on a mass basis (18 grams). These thicknesses correspond to an in-place initial density of 4.0 $lb/ft^3$ for the blended fiber beds and 0.9 $lb/ft^3$ for the pressure-washed fiber beds.

For each type of fiber preparation, the beds in the three head loss columns were fairly consistent with each other. For the blended fiber preparation, the thickness of the bed in each column was slightly different, with Column 1 having the thickest bed and Column 3 having the thinnest bed. The trend in thickness is consistent with the trend in accumulated head loss at the end of the test (i.e., Column 3 had the thinnest bed and the highest head loss). However, the differences were minor, as shown in Figure 11. Furthermore, the thickness of the debris beds did not change significantly over the duration of the test, even though the head loss changed dramatically for Columns 2 and 3, as noted earlier. The change in head loss over the duration of the tests cannot be attributed to the change in bed thickness, given that head loss is expected to vary linearly with bed thickness for a perfectly homogeneous debris configuration.

Similarly, the debris beds formed of NEI pressure-washed debris in the three columns were similar in overall thickness, but Column 2 had the thickest bed, followed by Columns 1 and 3, as shown in Figure 12. The top surface of the NEI pressure-washed debris beds was less uniform than for the blended fiber beds. The NEI pressure-washed debris beds were thicker in the center of the column and somewhat thinner at the edges where the debris bed touched the column wall.

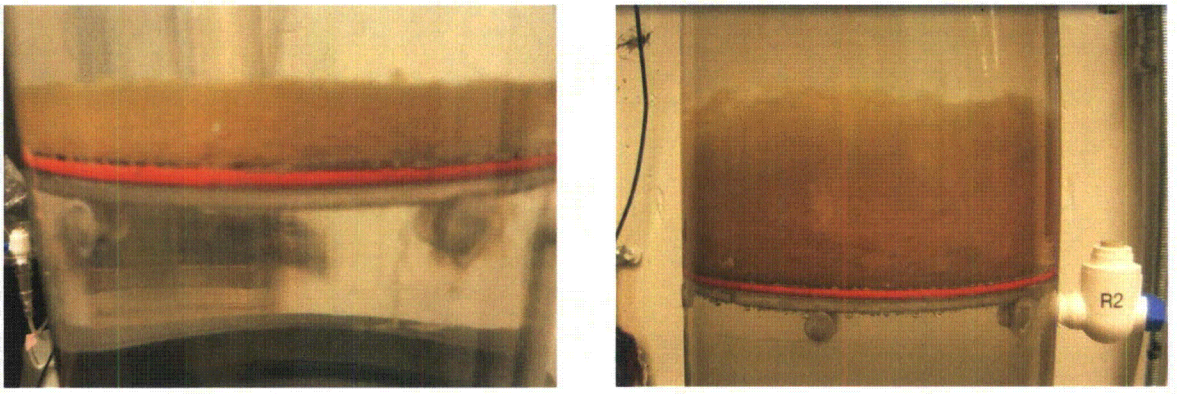


A B

**Figure 10: Debris beds in head loss columns at the beginning of test operation. (A) Column 2 blended fiber debris bed and (B) Column 2 NEI pressure-washed fiber debris bed.**

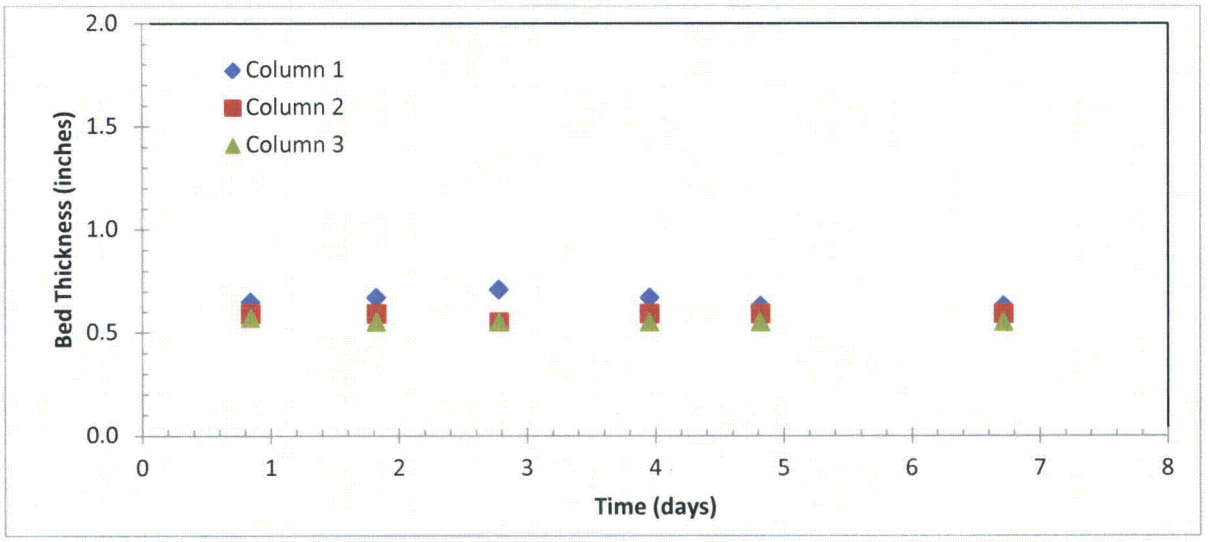


**Figure 11: Thickness of blended fiber debris beds in head loss columns.**

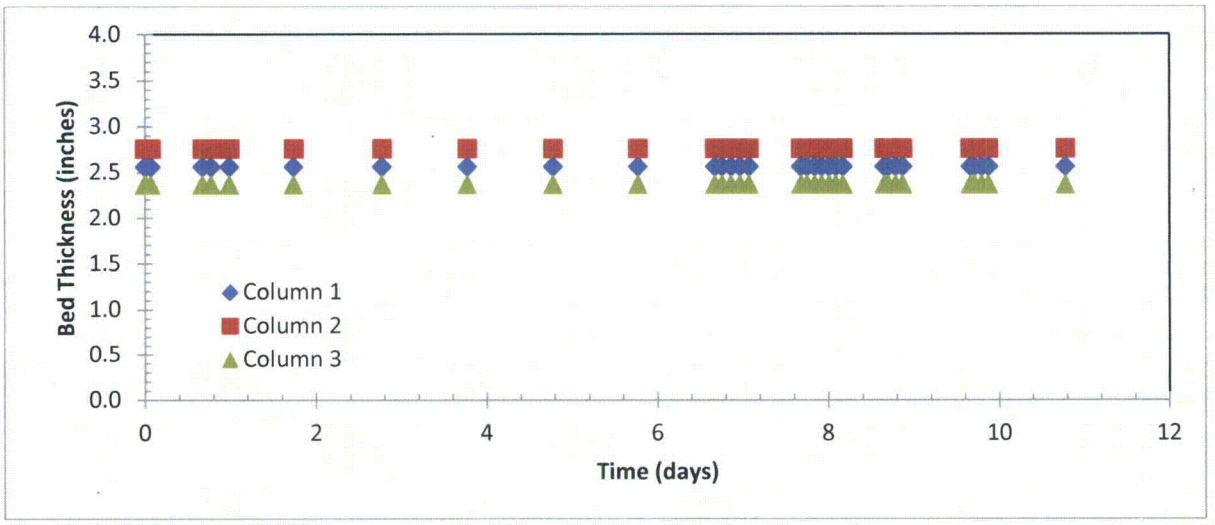


**Figure 12: Thickness of NEI pressure-washed fiber debris beds in head loss columns.**

Differences were also observed when the tests were complete and the debris beds were removed from the head loss columns. The blended fiber debris beds compressed slightly when water was removed from the column, from a thickness of about 0.6 inches (1.5 cm) to 0.4 inches (1 cm). After water was removed, water droplets falling from the inside of the column formed craters on the otherwise uniform surface of the blended fiber beds, as shown in Figure 13, indicating that the surface of the bed was soft and pliant.

As water was drained from the columns, the NEI pressure-washed debris beds collapsed more significantly, from about 2.6 inches (6.6 cm) to 0.8 inches (2 cm) in thickness. The surface of

the NEI debris beds was much rougher and less uniform after being removed from the column, as shown in Figure 13C.

A B C

**Figure 13: Photographs of the debris beds after the tests were complete. (A) Column 2 blended fiber debris bed in column after water was drained and clear section was removed from the test assembly (craters are from falling water droplets). (B) Column 2 blended fiber debris bed after being removed from column. (C) Column 1 NEI pressure-washed debris bed after being removed from column.**

After being removed from the head loss columns, the debris beds were stored in a dark refrigerated room at 4 °C until they could be examined in detail. For the blended debris beds, visual examination indicated the blended fiber beds to have a uniform, flat top surface. The craters from the water droplets in the bed from Column 3 appeared to have filled in over time and were less prominent than they had been when the bed was removed from the column. In all beds, the fibers were tightly packed so that the surface of the bed appeared similar to a piece of felt material. Individual fibers were not readily visible. Examination with a 16x magnification lens (Loupe) did not provide a significantly different view of the bed surfaces.

When a portion of the bed was torn from the surface and rubbed between two fingers, it stayed as an intact mat of fibers. However, the debris beds were easily torn and exhibited very little resistance when pulled apart by hand. The debris beds were cut vertically with a scissors, and the cross-section of the bed appeared uniform from top to bottom, also visibly similar to a piece of felt.

The most significant feature of the blended debris beds appeared at the bottom of the bed, where the debris bed was in contact with the perforated support plate. When the debris beds were peeled from the support plate, they exhibited nodules of fiber in a dimple pattern identical to the holes in the support plate. The bottom of the bed of all three columns with blended fiber preparation are shown in Figure 14. The texture of the nodules was significantly different from that of the fiber at the top or center of the debris bed. When rubbed between two fingers, the nodules were hard, almost as if a rock were embedded in the debris bed. When a nodule was pulled apart by hand, however, it offered no physical resistance and separated easily into a small mass of fibers with no evident larger solid materials. Visually, the nodules in bed 3 were darker than in bed 2, which were subsequently darker than in bed 1. The color might indicate that another material such as dirt was retained in the localized area of the fiber immediately at the perforated screen holding the debris beds. The debris beds appeared clean throughout their depth, as evidenced in the cross-section of the beds shown in Figure 14. The difference in the retention of dirt in the fiber at the perforated plate may have been the cause of the difference in

head loss among the three columns, being that the trend in color is consistent with the trend in head loss (darker color corresponding to greater head loss).

The dimple pattern evident at the bottom of the blended beds was barely evident on the NEI pressure-washed beds, as shown in Figure 15. These images indicate that the longer fibers present in the pressure-washed beds spanned the holes of the perforated screen differently, leading to different hydraulic conditions in the immediate vicinity of the support screen. The difference in fiber bed characteristics at the support screens appears to be a significant cause of the difference in head loss among the three columns for the blended fiber beds and between the blended fiber and pressure-washed columns.

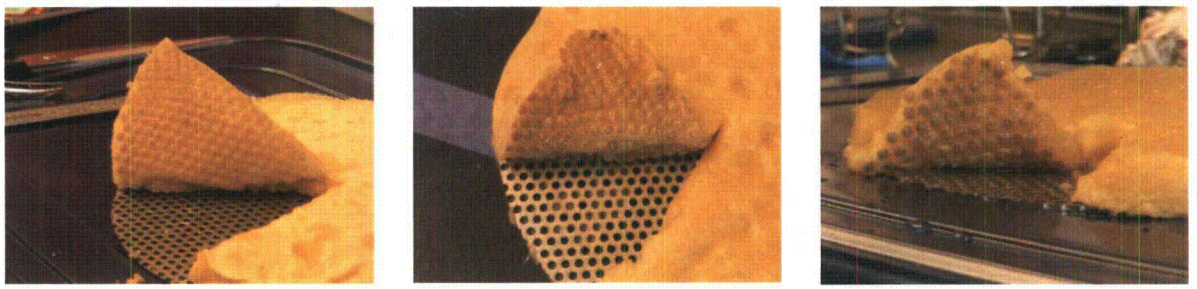

A B C

**Figure 14: Dimple pattern from the support plate on the bottom side of the blended fiber debris beds in (A) Column 1, (B) Column 2, and (C) Column 3. The dimples in Column 3 are darker than in Column 1. Also, the cross section of the debris bed, most evident on Column 3, appears clean throughout the entire depth of the debris bed.**

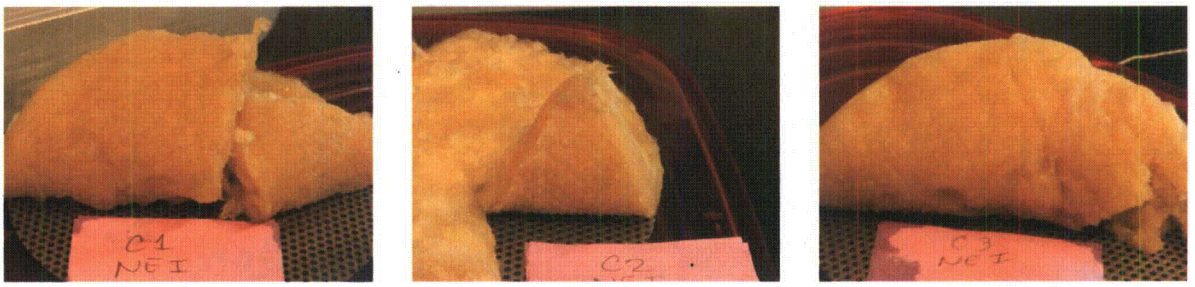


A B C

**Figure 15: Bottom side of the NEI pressure-washed fiber debris beds in (A) Column 1, (B) Column 2, and (C) Column 3.**

# Water Chemistry

## pH

The pH in the tank solution was measured using both an on-line pH probe and grab samples measured with a tabletop laboratory pH meter. The on-line probe was more difficult to calibrate than the laboratory pH meter and could not be calibrated while a test was in progress whereas the laboratory pH meter could be calibrated. The pH measurements by both the in-line probe and the laboratory pH meter are shown in Figure 16 for the blended fiber test and Figure 17 for the NEI fiber test. During the blended fiber test, the average pH was 7.35 using the on-line pH probe and 7.18 using the laboratory pH meter. The laboratory pH meter was calibrated each time it was used and was closer to the expected pH value of 7.2 based on calculations of the chemicals in the solution. The on-line probe was replaced with a new probe before the NEI test started. For the NEI fiber test, the average pH value was 7.13 using the on-line probe and 7.23 using the laboratory pH meter. Again, the laboratory pH meter was closer to the expected pH value of 7.2.

## Calcium and Silica

Calcium and silica were measured in the pool solution, along with the aluminum. The calcium results are shown in Figure 18 for the blended fiber beds and Figure 19 for the NEI fiber beds. The calcium concentration was fairly constant with time in both tests. In the blended fiber test, the calcium concentration was about 1.5 mg/L but in the NEI fiber test was somewhat higher, about 2.0 to 2.2 mg/L.

The silica results are shown in Figure 20 for the blended fiber beds and Figure 21 for the NEI fiber beds. The results were similar in both tests, starting at about 2.5 mg/L (after the TSP had been added to the tank and the solution had been circulating through the head loss columns for about 90 minutes) and gradually rising over a period of several days to a concentration of about 4.0 mg/L, where it stayed for the remainder of the tests.

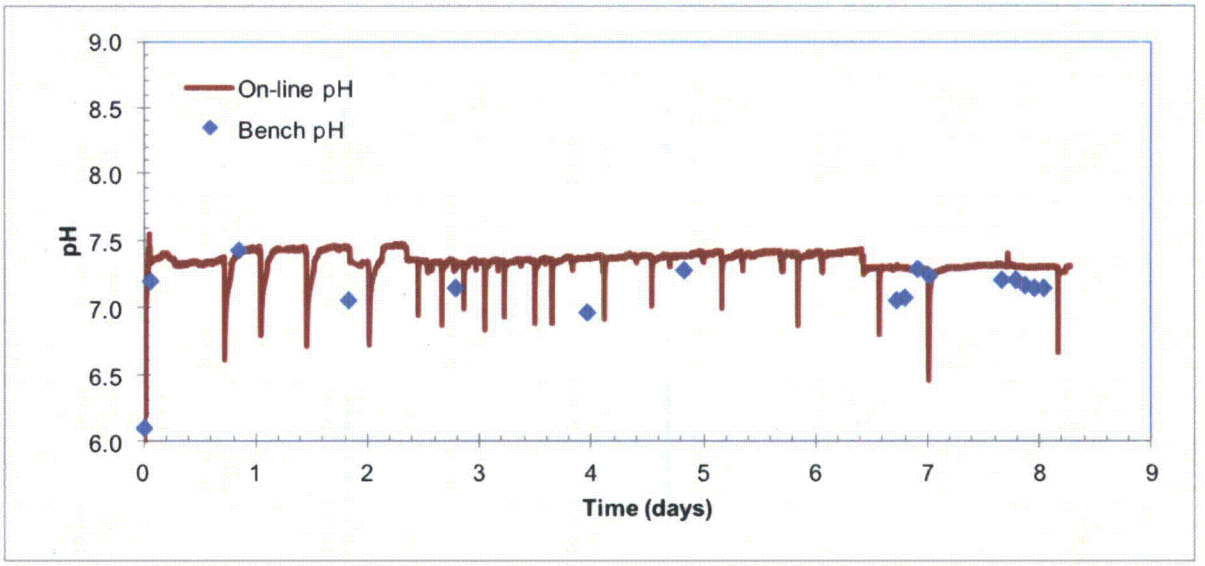


**Figure 16**: pH during the blended fiber test.

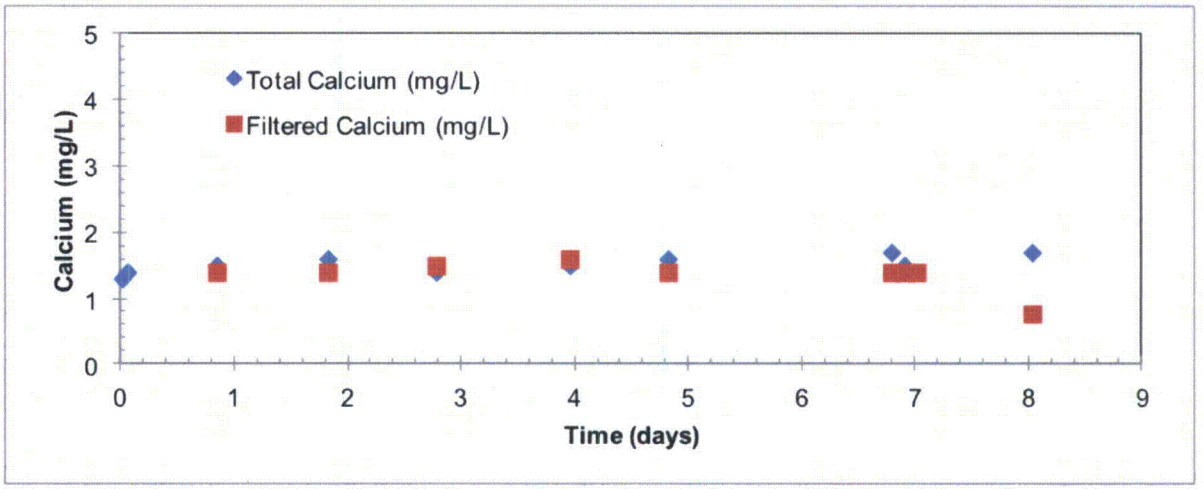


**Figure 17: pH during the NEI fiber test.**

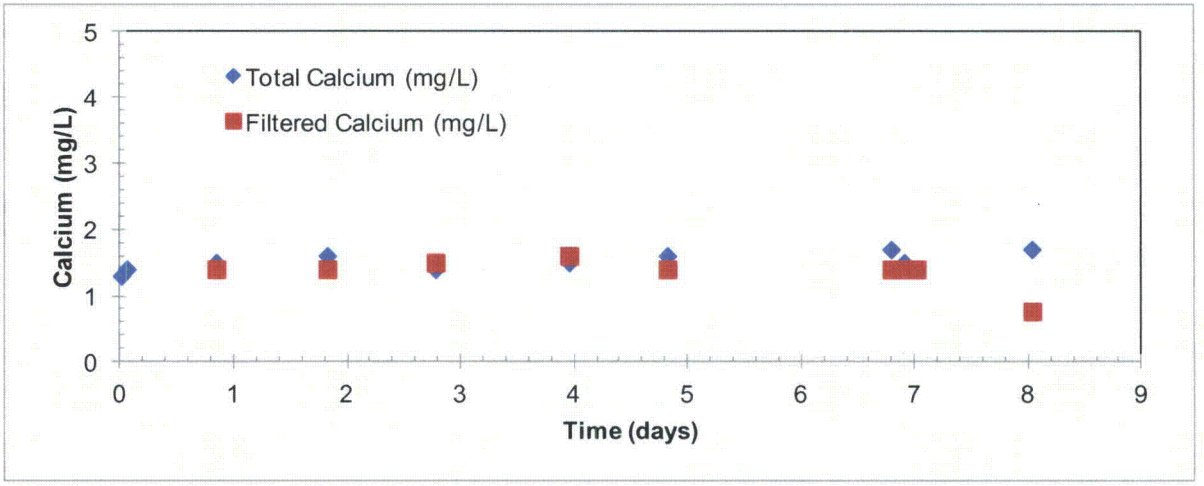


**Figure 18: Measured calcium in the CHLE pool solution during the blended fiber test.**

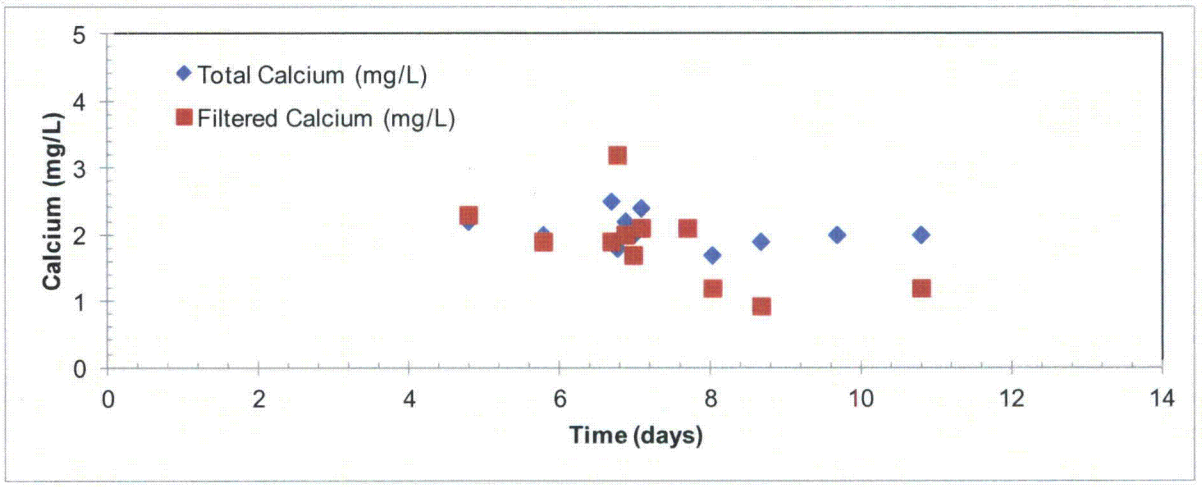


**Figure 19: Measured calcium in the CHLE pool solution during the NEI fiber test.**

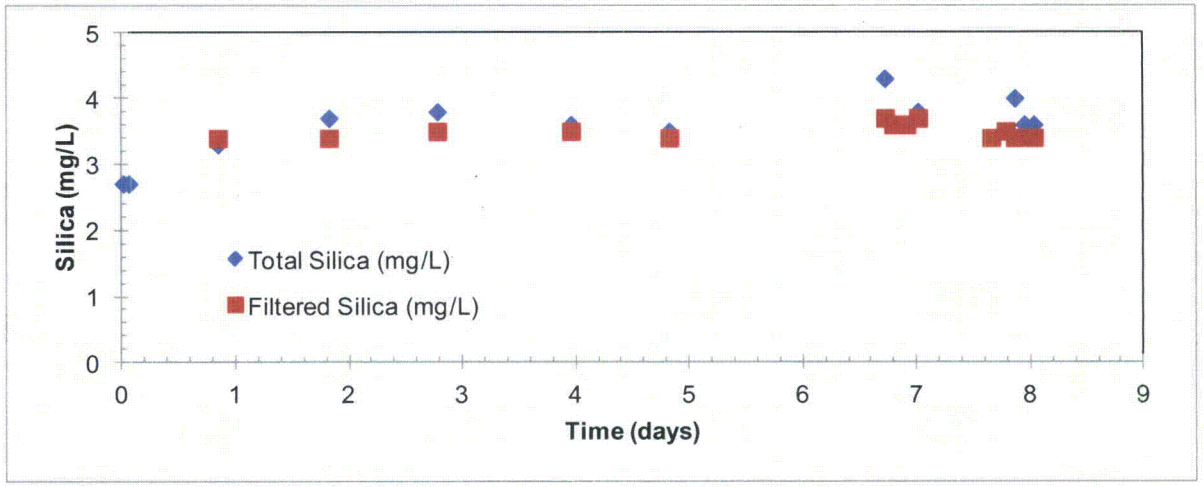


**Figure 20: Measured silica in the CHLE pool solution during the blended fiber test.**

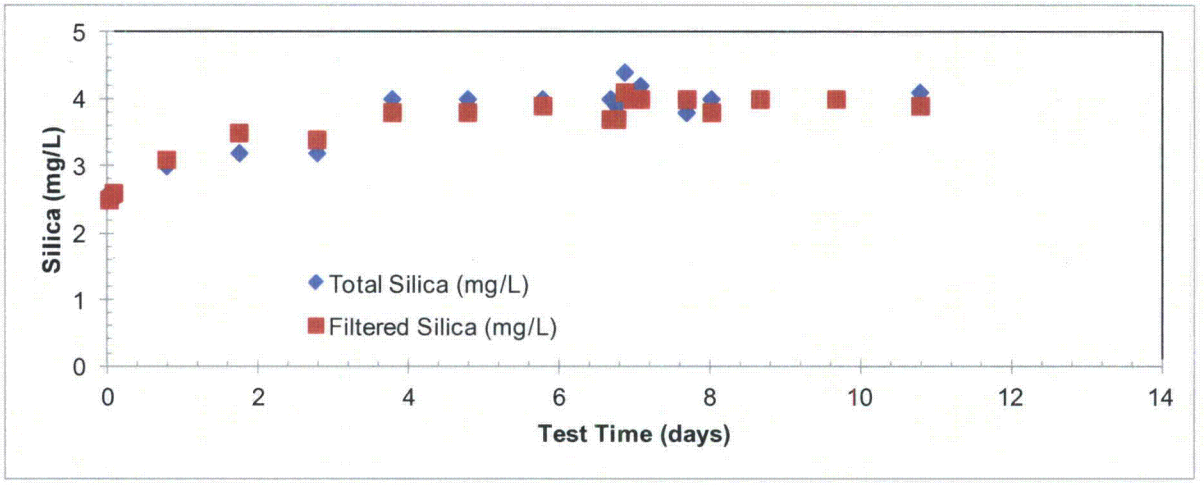


**Figure 21: Measured silica in the CHLE pool solution during the NEI fiber test.**

## Effect of Aluminum Addition

After 6.7 days of operation with no materials in the tank, aluminum nitrate were added to the tank in each test. Aluminum nitrate was added at a slow rate (an increase of 0.02 mg/L per minute) to minimize the potential for precipitation to occur due to localized high concentration at the point of injection. For the blender preparation method, aluminum addition continued until a concentration of 6 mg/L as Al was reached in the solution with, and the test was terminated when the head loss in two of the three columns exceeded 80 inches of water. No significant change in head loss was observed in the test with the NEI pressure-washed preparation method; therefore, the aluminum addition was added in 7 periodic batches until 40 mg/L as Al was reached in the solution.

### Turbidity

Several parameters were monitored as aluminum was added, including aluminum, calcium, and silicon concentrations in solution; total suspended solids; and turbidity. Determining the concentrations and suspended solids required sample analysis that took several days, but turbidity can be determined immediately. Turbidity correlated well with the formation of precipitates in the solution. In the test with the blended fiber, the turbidity started at about 0.81 NTU after the TSP was added and the CHLE tank was circulating through the head loss columns. Turbidity dropped slowly over several days, reaching 0.32 NTU on Day 6. After aluminum was added, the turbidity increased in direct proportion to the quantity of aluminum that was added, as shown in Figure 22. Turbidity is determined by measuring scattered light in a solution and is an indicator of particles in solution. Therefore, the turbidity is evidence that a precipitate was forming. Furthermore, the slight decrease in turbidity from 0.97 NTU after the first addition of aluminum was complete to 0.78 NTU before the second addition started (between days 7 and 8) may be an indication of removal of precipitates, possibly by being captured in the debris beds.

Similar results were observed for the test with the NEI fiber preparation. The turbidity started at about 0.63 NTU after the TSP was added and the CHLE tank was circulating through the head loss columns. The turbidity then dropped slowly, reaching 0.40 NTU on Day 6. After aluminum was added, the turbidity again increased in direct proportion to the quantity of aluminum that was added, as shown in Figure 23. The strength of this correlation indicates that essentially all of the aluminum that was being added was precipitating as particles in solution. The correlation between the amount of aluminum added and the turbidity in the solution for the NEI preparation method is shown in Figure 24.

## Aluminum Concentration

Samples were taken for total and filtered aluminum and analyzed by a commercial laboratory. The results of the analysis are shown in Figure 25 for the blended fiber beds and Figure 26 for the NEI fiber beds. In both cases, the total aluminum in solution agrees well with the amount of aluminum that was added in solution. However, the concentration of aluminum in the filtered samples is significantly lower. These results indicate that a portion of the aluminum was removed during the filtration process, as would be expected when precipitates form. However, in both cases, several mg/L of aluminum were measured in the filtered samples, indicating that not all of the precipitates that were detected by the turbidity measurements were removed by the laboratory filter. The standard filter for measuring filtered metals, however, has a nominal pore size of 0.45 µm. As will be shown later, evidence was found that the in-situ precipitates formed by the addition of aluminum nitrate were smaller than this size and a portion of the precipitates could have passed through the filter.

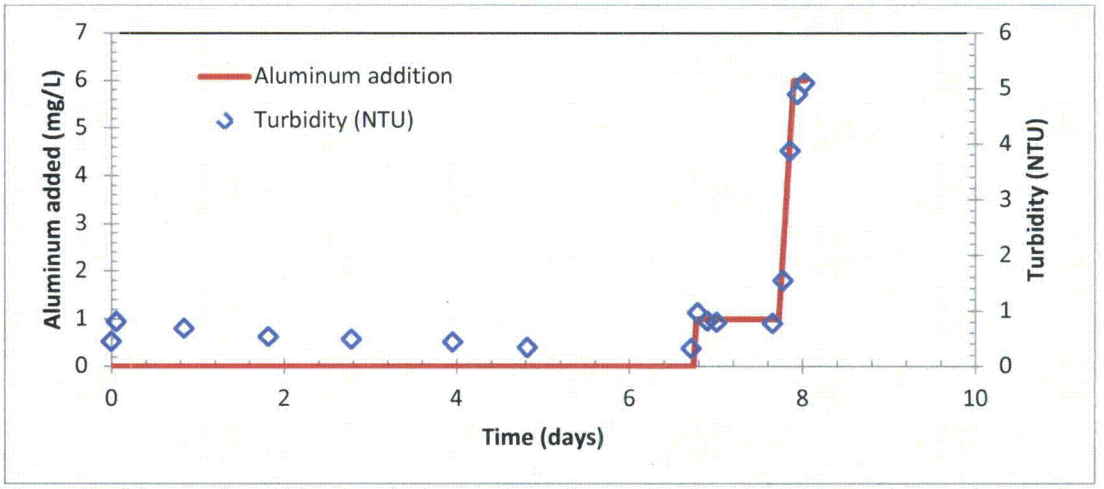


**Figure 22: Measured turbidity in solution, and aluminum added to the CHLE tank over time during test with blended fiber preparation.**

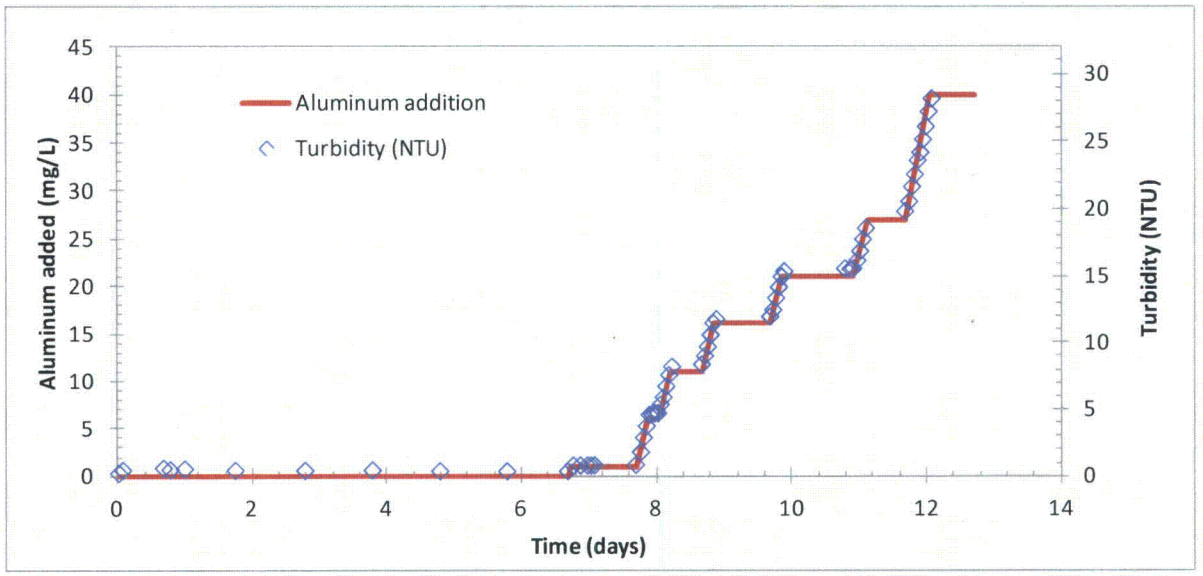


**Figure 23: Measured turbidity in solution, and aluminum added to the CHLE tank over time during test with NEI pressure-washed fiber preparation.**

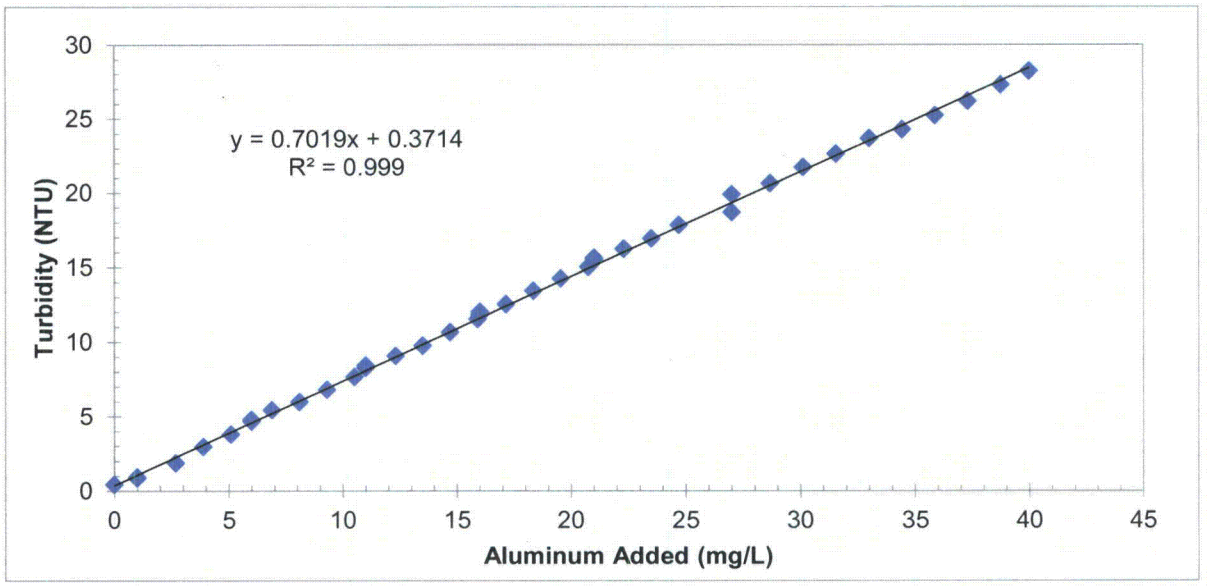


**Figure 24: Correlation between measured turbidity in solution and amount of aluminum added to the CHLE tank in the form of aluminum nitrate.**

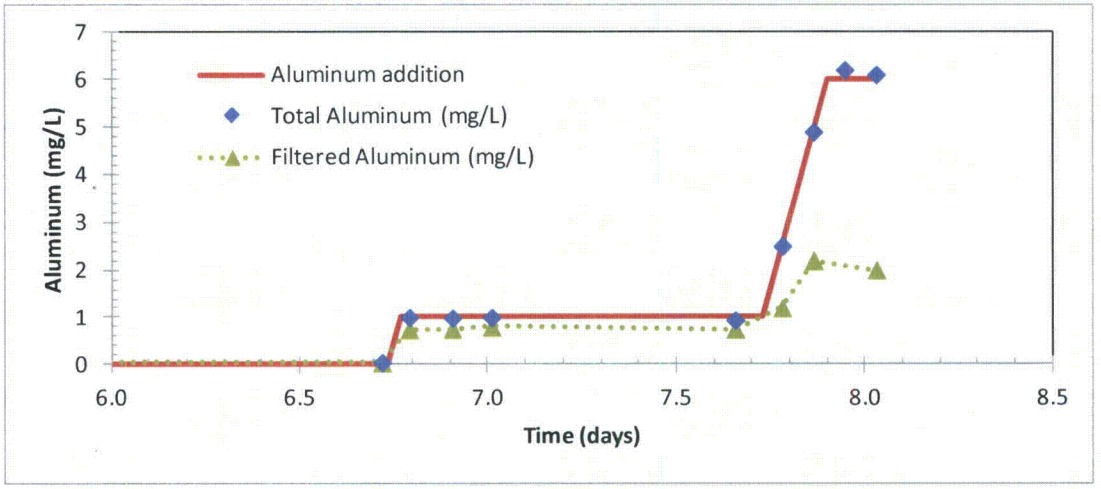


**Figure 25: Measured total and filtered aluminum concentration in the CHLE pool solution during the blended fiber test, along with the aluminum that was added.**

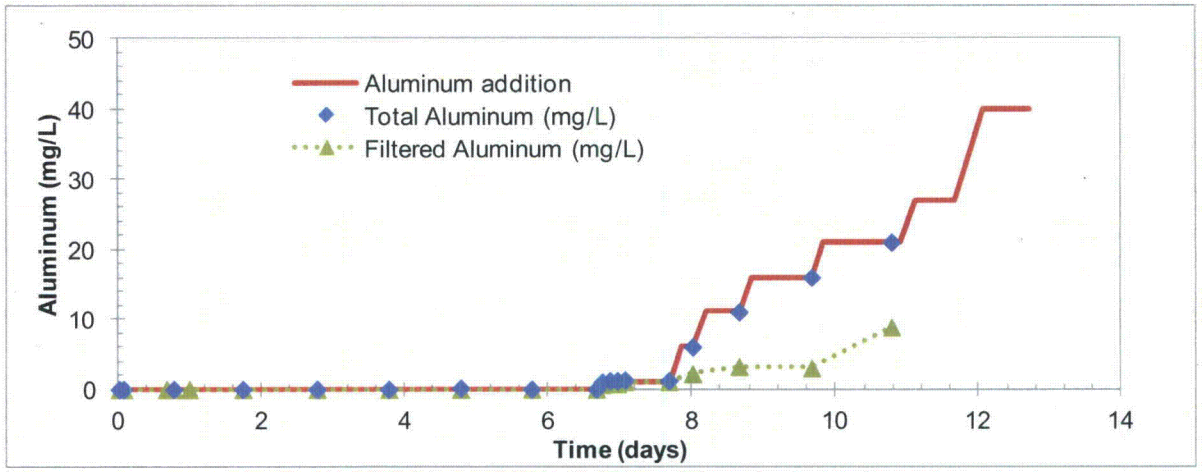


**Figure 26: Measured total and filtered aluminum concentration in the CHLE pool solution during the NEI fiber test, along with the aluminum that was added.**

## Total Suspended Solids

Total suspended solids (TSS) was a less reliable indicator of the presence of precipitates than turbidity was. The TSS results are shown in Figure 27 for the blended fiber beds and Figure 28 for the NEI fiber beds. The factor most likely contributing to the poor correlation between TSS and precipitation formation was the particle size of the precipitates relative to the nominal pore size of the filter. The filter used for the TSS analysis is a glass-fiber filter with a nominal pore size of 1.2 µm (Whatman GF/C). As will be demonstrated later, the precipitates had an average size smaller than that, and many of the particles may have passed through the filter without having been measured as suspended solids. Prior to the addition of aluminum nitrate, the TSS of the solution was between 3 and 5 mg/L for both tests.

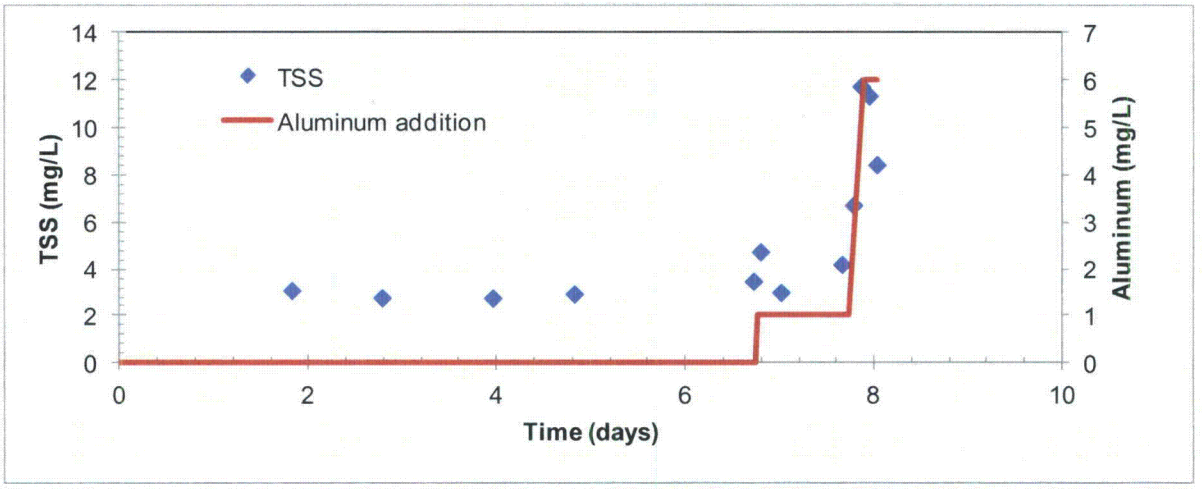


Figure 27: **Measured total suspended solids (TSS) in the CHLE pool solution during the blended fiber test, along with the aluminum that was added.**

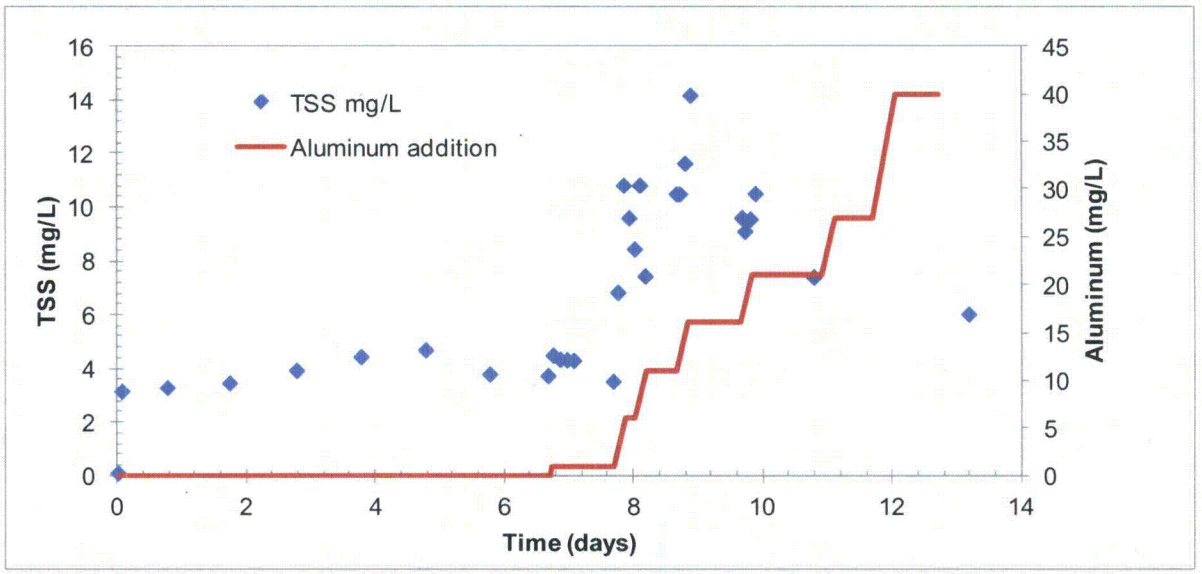


**Figure 28: Measured total suspended solids (TSS) in the CHLE pool solution during the NEI fiber test, along with the aluminum that was added.**

## Debris Bed Head Loss

The head loss trends after the aluminum was added to the blended fiber beds are shown in Figure 29. After 1 mg/L of aluminum had been added, the head loss in all three columns started increasing. After 12 hours of operation, Column 3 reached its maximum head loss and its operation was terminated. The following day, 5 mg/L of aluminum was added (yielding a total of 6 mg/L). The head loss in Columns 1 and 2 started increasing rapidly, and the test was terminated after an additional 6 hours. Details of the statistical significance of the change in head loss after aluminum was added is described in Appendix A.

Previous tests were conducted by adding pre-formed WCAP precipitate directly to the CHLE tank in batches. These tests were previously summarized in CHLE-008. The results of a test with WCAP precipitate and blended fiber beds are shown in Figure 30. The tests with in-situ precipitate formation and WCAP precipitate addition are difficult to compare because the latter had larger quantities of precipitate added over shorter periods of time. In addition, the tests in this series had been exposed to circulating solution for over 6 days, which may have led to sufficient local compaction to permit a more rapid response to the aluminum nitrate compared to the earlier tests. In the WCAP tests, five batches of WCAP precipitate, totaling 21.8 mg/L of aluminum, were added over a 4-hour period. Head loss started increasing rapidly about 4 hours after the first addition of WCAP precipitate, and the test was terminated an hour later. However, it is evident that in the case of blended fiber beds, both in-situ precipitate formation and the addition of pre-formed WCAP precipitates can cause significant head loss. It should be noted that the timing of head loss generation can be influenced by physical arrangement of debris in the bed and the degree of compaction that has been allowed to occur prior to the chemical arrival.

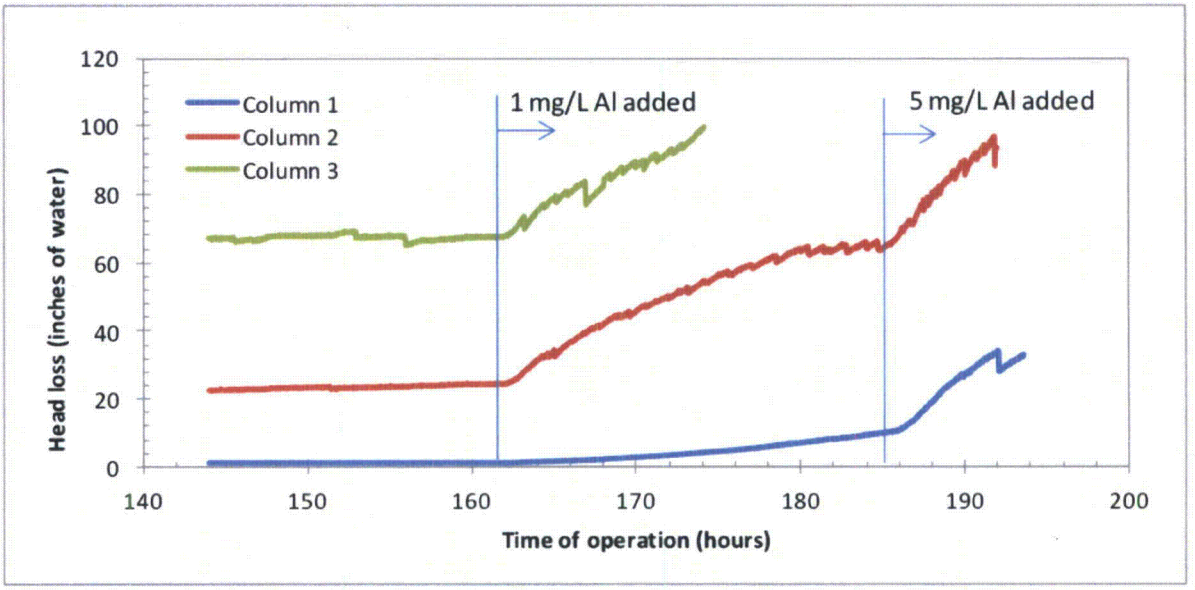


**Figure 29: Head loss through debris beds with blended fiber preparation when in-situ precipitation occurred due to the addition of aluminum nitrate to the CHLE tank.**

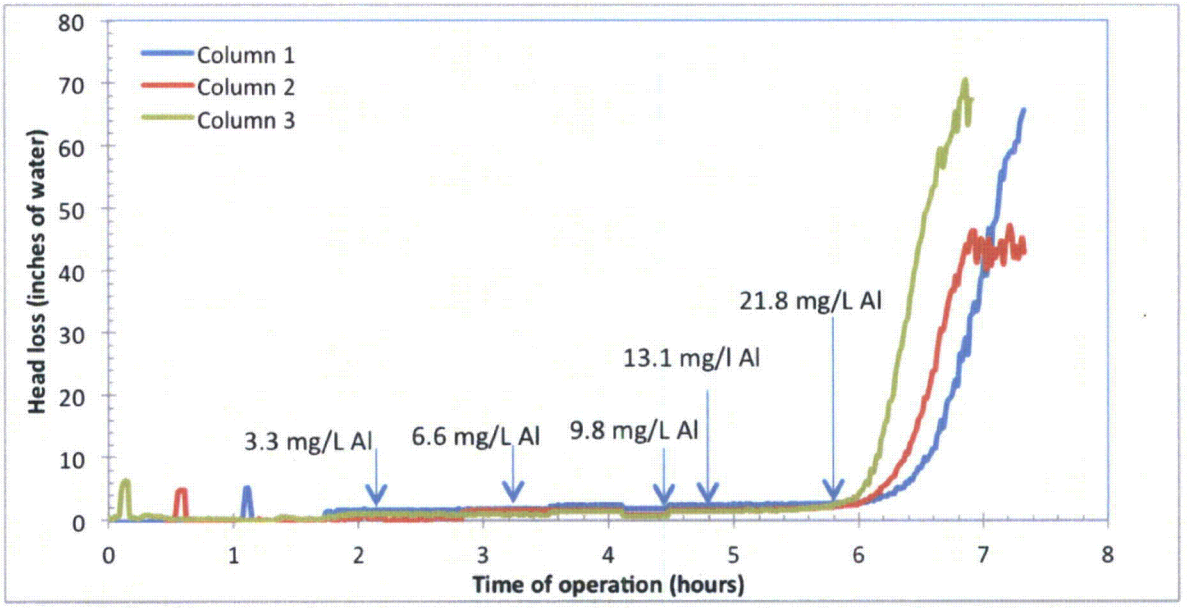


**Figure 30: Head loss through debris beds with blended fiber preparation when pre-formed WCAP precipitates were added to the CHLE tank.**

Significantly different results were obtained when in-situ precipitation was achieved in the tests with NEI pressure-washed fiber preparation. The initial 1 mg/L and 5 mg/L aluminum additions did not cause any change in head loss. Thus, head loss additions continued daily for several additional days, until a total of 40 mg/L of aluminum had been added to the solution. The aluminum addition and head loss results are shown in Figure 31. Column 2 had a change in performance after 16 mg/L of aluminum had been added, and this change in performance was determined to be statistically significant, as described in Appendix A. However, the change appears to be in the range of 0.1 inches of water, a change in head loss that would not be considered problematic during a LOCA. No statistically significant changes in head loss occurred in Columns 1 and 3 even after 40 mg/L of aluminum had been added.

Figure 32 shows that the NEI pressure-washed fiber beds behaved significantly differently when pre-formed WCAP precipitates were added to the CHLE tank. The same quantity of aluminum (40 mg/L) was added in the form of WCAP precipitates, except that it was added in a much shorter period of time (about 2 hours for WCAP versus about 5 days for the in-situ precipitate formation) and the WCAP was added in three batches versus seven addition cycles for the in-situ precipitate formation. However, when WCAP precipitates were added, the debris beds rapidly reached their maximum head loss values. When the same amount of aluminum was added to cause in-situ precipitation, no head loss occurred over a period of days, despite that the same type of debris beds (NEI pressure-washed) were present, and with the same quantity of fiber (18 g per bed). A comparison of Figures 31 and 32 is evidence that the slow formation of precipitates in-situ due to the addition of aluminum nitrate over a period of days into a buffered, borated solution typical of a LOCA at STP is not the same as the precipitates that are formed by the WCAP protocol. The same addition of aluminum caused over 80 inches of water of head loss when added as the WCAP precipitate, versus less than 1 inch of water of head loss when

formed as an in-situ precipitate. It is important to understand the physical mechanisms that permit NEI fiber to pass in situ chemical products compared to the significant filtration of WCAP material.

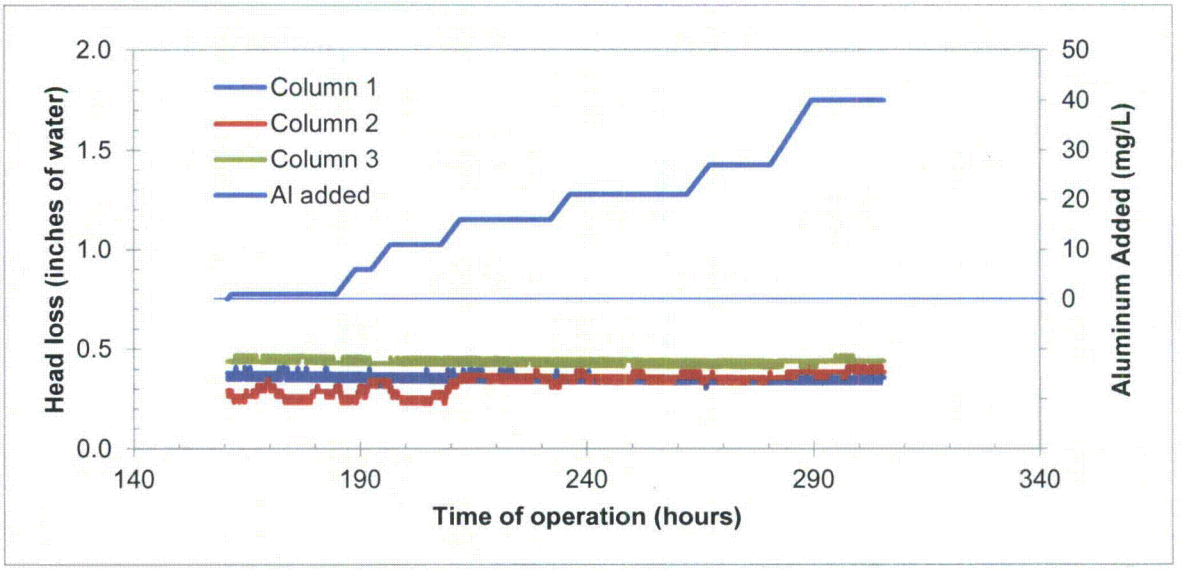


**Figure 31: Head loss through debris beds with NEI pressure-washed fiber preparation when in-situ precipitation occurred due to the addition of aluminum nitrate to the CHLE tank.**

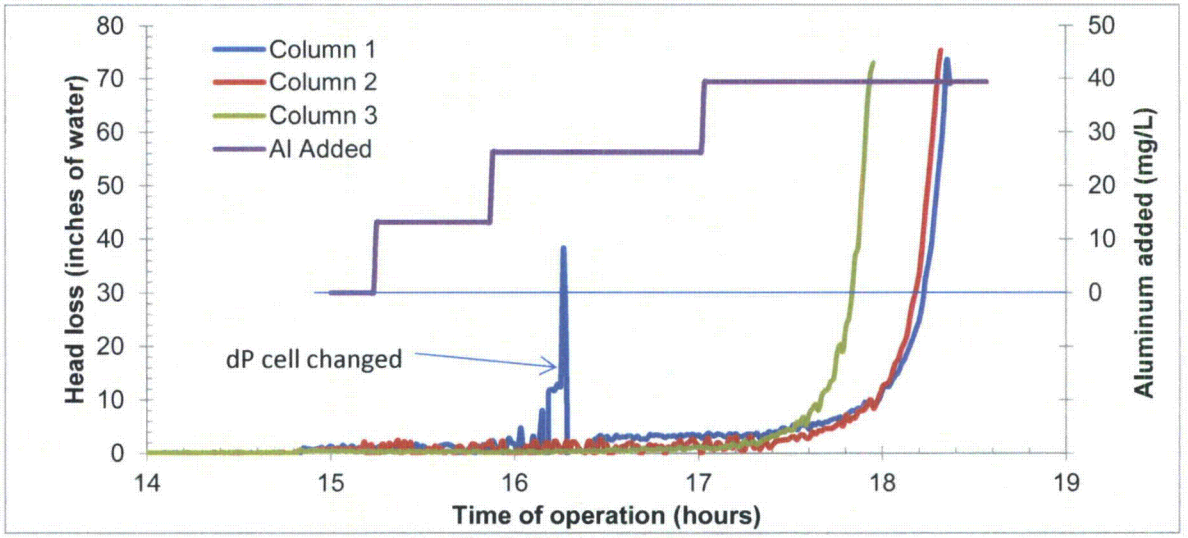


**Figure 32: Head loss through debris beds with NEI pressure-washed fiber preparation when pre-formed WCAP precipitates were added to the CHLE tank.**

## Particle Size and Zeta Potential

To determine the cause of the difference in performance of the in-situ and pre-formed WCAP precipitates, the particle size and zeta potential of the precipitates were measured. The zeta potential is a measure of the surface charge of particles, which can affect their ability to aggregate into larger particles or to be retained in a filter. The analysis revealed distinct differences between the in-situ and pre-formed WCAP precipitates. The particle size and zeta potential measurements are summarized in Table 2. The preformed WCAP precipitates had a particle size of about 1.6 µm when they were in a solution containing boric acid and TSP at the concentrations used in the CHLE tests. This size was consistent over three samples of WCAP precipitates. When the WCAP precipitates were placed in a solution containing water that had been deionized by reverse osmosis, the particle size was slightly larger, ranging from 1.8 to 2.5 µm. This difference in size is unlikely to make a substantive difference in how the particles behave in solution or their ability to be retained in a debris bed. When the WCAP precipitates were placed in a solution containing tap water, the particle size was about the same size, 1.2 µm.

An important result in Table 2 is the size of the in-situ precipitates. These precipitates were measured at 0.17 µm on the day that the NEI test was completed. This size is one-tenth that of the pre-formed WCAP precipitates. The substantial difference in size may help explain why the pre-formed WCAP precipitates were retained by the NEI fiber beds but the precipitates formed in-situ were not. Samples of solution from the NEI test were stored in a laboratory oven at the final temperature of the test (40 °C) for two weeks, after which the particle size was measured again. The particle size was virtually identical in the second measurement, indicating that no aggregation had taken place over the storage period. In addition, visual observation indicated that no settling had occurred over the storage period, which is consistent with the small size of the particles.

Table 2: Particle size and zeta potential of aluminum hydroxide precipitates [1]

| | Particle Size (µm) | Zeta Potential (mV) |
|---|---|---|
| Pre-formed WCAP Precipitates | | |
| In boron/TSP water, 30 mg/L dilution | 1.6 | -28 |
| In boron/TSP water, 40 mg/L dilution | 1.6 | -25 |
| In boron/TSP water, 10 mg/L dilution | 1.6 | -27 |
| In deionized water, 40 mg/L dilution | 1.8 | 29 |
| In deionized water, 10 mg/L dilution | 2.5 | 30 |
| In tap water | 1.2 | -3 |
| | | |
| In-situ Precipitates (in boron/TSP water) | | |
| At end of test | 0.17 | -31 |
| Two weeks later | 0.18 | -32 |

1. Each value given is the average of three measurements

When precipitates were placed in water containing boric acid and TSP, they had a zeta potential ranging from -25 to -32, regardless of whether they were pre-formed WCAP precipitates or in-situ precipitates. The in-situ precipitates were slightly more negative than the pre-formed WCAP

precipitates. When particles are retained in a debris bed entirely by mechanical sieving, the charge on the particles is not important. However, when particles are smaller than the void dimensions in the debris bed, surface charge can have a significant impact on particle retention. Particles that have similar charge to the media in the debris bed will have electrostatic repulsion with the media and are less likely to be retained. Particles that are neutral or have opposite charge to the media can be retained by van der Waals forces or by electrostatic attractive forces.

Previous work by Duke Energy indicated that Nukon fibers are also negatively charged, although the magnitude of the charge depended on the solution in which the fibers were immersed. At a pH of about 7, that report found that Nukon fibers had a zeta potential of about -25 in water containing boric acid but about -12 in either deionized water or tap water. The report by Duke Energy noted that head loss through fiber beds could be a function of the type of water used, and attributed some of the difference in head loss performance to the zeta potential.

Because the in-situ particles and the Nukon fiber both have significant negative charge when immersed in water containing boric acid and TSP, they will have repulsive electrostatic forces and will not be retained unless the void dimensions in the debris bed are small enough to physically sieve the particles. These effects may explain the differences between the blended and NEI debris beds. The blended beds had hard nodules of fiber adjacent to the perforated screen, and these nodules had apparently retained some dirt or other material, leading to a difference in head loss among the three columns. The nodules apparently had small enough void dimensions that they were able to retain both pre-formed WCAP precipitates and in-situ precipitates. The NEI fiber bed, however, did not have the hard nodules of fiber and had void spaces small enough to retain the pre-formed WCAP precipitates but not small enough to retain the in-situ precipitates, which were one-tenth the size.

The results in Table 2 also indicate that the zeta potential of pre-formed WCAP precipitates was dependent on solution chemistry. In water containing boric acid and TSP, the precipitates were negatively charged with a zeta potential around -27. In tap water, the precipitates were nearly neutral with a zeta potential around -3. In deionized water, the precipitates were positively charged with a zeta potential around +30. These results could be significant for the use of pre-formed WCAP precipitates for some head loss tests. If debris beds are formed that are porous enough that they do not physically sieve precipitates, pre-formed WCAP precipitates that are used in tests containing deionized water or tap water are likely to be retained in the debris bed by electrostatic attraction or van der Waals attractive forces. In contrast, if the tests used water containing boric acid and TSP, the precipitates would be less likely to be retained because of the repulsive electrostatic forces, and less head loss would occur. Neither deionized nor tap water conditions exist within the post LOCA accident environment, so negative repulsive forces are likely to exist between fiberglass debris and aluminum based chemical products that may form in the sump environment.

## Conclusions

The tests described in this report were developed to investigate (1) the suitability of debris beds for use in long-term corrosion/head loss experiments, which may be up to 30 days long, and (2)

the response of the debris beds to the slow addition of aluminum nitrate, which can simulate the release of aluminum into solution by corrosion.

The fiber beds prepared with blending in a blender were not reproducible between columns. After 6 days of operation, the head loss varied from 1.2 inches of water to 61 inches of water through debris beds that were circulating the same water at the same rate. The lack of reproducibility would make it difficult to use this fiber bed preparation method in the CHLE program to assess the importance of chemical effects, because the difference in performance of due to variability may be greater than the difference in performance due to the addition of chemical effects. The lack of reproducibility of the fiber beds with the blended preparation appears to be due to localized regions of more dense fiber packing immediately adjacent to the perforated support plate.

In contrast, the fiber beds prepared with the NEI pressure-washing method were reproducible between columns and had steady performance over time. Testing by an outside laboratory demonstrated that the NEI pressure-washing method results in longer fibers. The shorter "shards" of fibers in the blended beds may be a key reason for the irreproducibility of those debris beds.

When aluminum nitrate was introduced into the solution, precipitates formed, as evidenced by turbidity measurements. There was a strong correlation between the turbidity measurements and the amount of aluminum that had been added. After aluminum nitrate was introduced into the solution, the head loss through the blended fiber beds increased. For the NEI pressure-washed debris beds, one of the three beds had a statistically significant response to the addition of aluminum nitrate, but the change in head loss was only about 0.1 inches of water in that column, which is not enough to cause concern during a LOCA. The other two NEI pressure-washed debris beds did not have a statistically significant response to the addition of aluminum nitrate, even though in earlier tests they did experience a significant increase in head loss after pre-formed WCAP precipitates were added to the system.

Particle size analyses indicate that the size of precipitates formed in-situ are up to 10 times smaller than the pre-formed WCAP precipitates with similar solution conditions (0.17 μm versus 1.6 μm in diameter). This significant difference in size appears to be sufficient to cause the pre-formed WCAP precipitates to be retained by the NEI fiber debris beds but allow the in-situ precipitates to pass through the NEI fiber debris beds. The results indicate that head loss may be less significant than indicated by the use of pre-formed WCAP precipitates, depending on the filtration characteristics of the debris bed.

Zeta potential analyses indicate that solution chemistry affects the surface charge of pre-formed WCAP precipitates. When tests were conducted in deionized water, pre-formed WCAP precipitates had a positive zeta potential. When tests were conducted in Albuquerque tap water, the pre-formed WCAP precipitates were nearly neutral. When tests were conducted in water containing boric acid and TSP, the precipitates had a significant negative charge. The reversal of charge depending on solution chemistry suggests that head loss testing using pre-formed WCAP precipitates may not adequately predict the extent of head loss through a strainer under conditions in which debris beds are not reliant on physical sieving for the retention of particles.

Despite the slow introduction of aluminum nitrate, corrosion conditions may not have been perfectly emulated in these tests. It is possible that conditions that minimize aluminum release, such as the passivation of aluminum surfaces or the formation of a low-solubility oxide layer, would result in an upper limit to the aluminum concentration measured in solution. In addition, saturation conditions relevant for direct nucleation of precipitation products within the fiber bed may have been artificially exceeded. If direct nucleation is a credible formation mechanism, then the tests reported here best describe the filtration behavior between the two preparation methods and not necessarily the in-situ head-loss sensitivity. Direct nucleation would avoid the complications of particle filtration, perhaps leading to different head loss response in the NEI pressure-washed debris beds. As a result, additional tests that investigate precipitate formation under prototypical corrosion conditions are needed.

It is important to note that a growing suite of routine diagnostics is available to detect and characterize the presence of chemical products. These tests include: optical turbidity, analytical measurements of solution chemistry, particle sizing, zeta potential, SEM fiber examination, chemical addition mass balance, online differential pressure, and visual estimation of debris beds. There is no exclusive dependency on differential pressure to detect the presence of chemical products. The use of several of these experimental methods can be used to detect the presence of chemical precipitates in an integrated corrosion/head loss test to evaluate whether precipitates that may form following a corrosion process are similar to the precipitates detected here after the addition of aluminum nitrate. In addition, the tests can be coupled with the use of NEI pressure-washed debris beds in the head loss columns to determine whether the head loss characteristics in response to direct nucleation of precipitates in the fiber bed are similar to the response of precipitates that form after the addition of aluminum nitrate.

## References

1. Nuclear Energy Institute (NEI). "ZOI Fibrous Debris Preparation: Processing, Storage, and Handling, Revision 1", January 2012.
2. Ruland, W.H. Letter to John Butler of the Nuclear Energy Institute with the subject line "Fibrous Debris Preparation procedure for Emerengy Core Cooling System Recirculation Sump Strainer Testing, Revision 1" dated April 26, 2012.
3. University of New Mexico (UNM). "CHLE-008 Debris Bed Formation Results, Rev 3", June 2012.
4. IPD Testing Experts. "Test Report: Report to Timothy Sandy of Alion Science and Technology" dated July 26, 2012.

# Appendix A - CHLE Tank Test Results for Blended and NEI Fiber Beds with Aluminum Addition: Correlated Control Charts for Head Loss Response to Aluminum Addition

# CHLE Tank Test Results for Blended and NEI Fiber Beds with Aluminum Addition: Correlated Control Charts for Head Loss Response to Aluminum Addition

by Jeremy Tejada and David Morton, The University of Texas at Austin

August 17, 2012

## 1. Summary of Analysis

We develop and analyze control charts for the head loss data in Report CHLE-010: CHLE Tank Test Results for Blended and NEI Fiber Beds with Aluminum Addition (Howe, 2012). Table 1 summarizes the results that we describe in detail in subsequent sections. The analysis consists of assessing the performance of control charts for head loss for three columns using, in turn, three CHLE head loss columns for the NEI fiber beds and three CHLE head loss columns for the blended fiber beds.

| | **NEI Fiber Bed** | **Blended Fiber Bed** |
|---|---|---|
| **Column 1** | Lack of evidence suggesting change in head loss process after addition of aluminum. | Strong statistical evidence of change in head loss process after aluminum is added. |
| **Column 2** | Statistically significant change in head loss process after addition of aluminum. Conclusion based violations of upper control limit over multiple half-day time periods. | Strong statistical evidence of change in head loss process after aluminum is added. |
| **Column 3** | Lack of evidence suggesting change in head loss process after addition of aluminum. | Statistically significant change in head loss process after addition of aluminum. Conclusion based violations of upper control limit using half-day moving average. |

Table 1. Summary of Results of Analyzing Control Charts for Temperature-corrected Head Loss Process in Three Columns using NEI Fiber Bed and Blended Fiber Bed.

## 2. Introduction

The objective of this analysis is to determine whether the addition of aluminum over time caused a statistically significant response in terms of head loss through the debris beds. The experiment was

designed to record data each minute, with each data point being the average of six measurements during that minute. Thus, the data from the experiment forms a time series where the (average) head loss through the debris bed is provided for each minute over several days of experimentation. The experiment used three identical physical, vertical columns, and data are provided for each column separately. Thus we perform the analysis we describe on each column separately. We report analysis for six data sets: Three CHLE head loss columns for the NEI fiber beds and three CHLE head loss columns for the blended fiber beds. In order to assess whether we observe a statistically significant response in head loss due to the addition of aluminum over time, we use control charts. Specifically, we use control charts designed to handle correlations and trends in time series data (Croux et al., 2010). We organize the remainder of this analysis as follows: Section 3 presents some of the details of the time series control charts that we use, and Sections 4 and 5 present the results for the NEI fiber beds and the blended fiber beds, respectively, along with a brief discussion of these results.

## 3. Control Charts for Time Series Data

In this section, we present some of the details for a control chart for a time series, $\{y_t\}$, and our description follows closely that of Croux et al. (2010). At each point in time we obtain a one-step-ahead forecast using the Holt-Winters forecasting algorithm, and we plot the errors from this one-step-ahead forecast on a control chart. We construct the control limits to monitor new observations from a training sample, and we use the one day (1440 minutes) before aluminum was added in the experiment as our training period, as we assume the error process has reached a steady state by this point (about 5.8 days into the experiment).

### 3.1. Holt-Winters Forecasting Algorithm

Assume we have observed a time series up to time period $t-1$. The Holt-Winters method predicts the series at time $t$, which we denote $\hat{y}_{t|t-1}$. After we observe the actual value, $y_t$, we compute the one-step-ahead forecast error $e_t$ according to

$$e_t = y_t - \hat{y}_{t|t-1}. \tag{1}$$

We denote the level of the time series by $\alpha_t$, and the trend in the series by $\beta_t$. The Holt-Winters method for estimating these values after each realization, $y_t$, is as follows

$$\hat{\alpha}_t = \lambda_1 y_t + (1-\lambda_1)(\hat{\alpha}_{t-1} - \hat{\beta}_{t-1}) \tag{2}$$

$$\hat{\beta}_t = \lambda_2(\hat{\alpha}_t - \hat{\alpha}_{t-1}) + (1-\lambda_2)\hat{\beta}_{t-1} \tag{3}$$

and this results in the forecast

$$\hat{y}_{t+1} = \hat{\alpha}_{t-1} + \hat{\beta}_{t-1}. \tag{4}$$

The parameters $\lambda_1$ and $\lambda_2$ in (2)-(3) are smoothing parameters that take on values between zero and one. Larger parameters values lead to less smoothing and more weight being placed on the current values opposed to the previous level and trend. The relations (2)-(3) begin after a warm up period, in our case about 5.8 days. A linear model is fitted to the warm-up data in order to determine estimates of the initial level $\alpha_0$ and trend $\beta_0$. After the warm-up period, there is a training period, in our case 1 day or 1440 minutes. We determine the values for the smoothing parameters $\lambda_1$ and $\lambda_2$ by minimizing the sum of squared forecast errors over a training period as follows:

$$(\lambda_1^{opt}, \lambda_2^{opt}) \in \underset{(\lambda_1,\lambda_2)}{\arg\min} \sum (y_t - \hat{y}_{t+1})^2. \tag{5}$$

A simple two dimensional guess-and-check search over these parameter values can provide the optimal values to within two decimal places very quickly.

### 3.2. Control Chart

We monitor and plot the one-step ahead forecast errors on the control chart in order to determine if, and when, the process goes out of statistical control. As with most control charts, we assume the forecast errors (not the data itself) are normally distributed. The upper control limit (UCL) and lower control limit (LCL) are set using the forecast errors during the training period. We denote the mean of the squared prediction errors in the training period by

$$S^2 = \frac{\sum e_t^2}{n}, \tag{6}$$

where $n$ is the number of data points in the training period. The target value for the forecast errors is zero, so the $(1-\alpha)$-level UCL and LCL are:

$$\begin{aligned} UCL &= z_{\alpha/2} * S \\ LCL &= -z_{\alpha/2} * S \end{aligned} \tag{7}$$

where $z_{\alpha/2}$ is the $(1-\alpha/2)$-level quantile of the standard normal distribution.

For each new observation in the test period, the recursive relations (2)-(3) are updated, and the forecast error for that observation can be computed and plotted on the control chart. If it falls outside the limits, its value is statistically significantly different from the predicted value, indicating some unexpected changed in the process. Observations that are part of the test period influence future forecast errors via the Holt-Winters forecast formulas as these are continually updated. However, these observations do not alter the control limits.

In what follows, we build two-sided control charts as we describe above, using (7). That said, we have interest in increases in head loss, and so we pay particular attention to violations of the upper control limit in equation (7). Some violation of that control limit is expected, even if the system remains "in control" due to the statistical nature of the process. Such violations of the upper control limit would occur at rate $\alpha/2$. For this reason, when a more nuanced analysis is needed (Section 4 and Section 5.3), we track a moving average of the rate of violation to help assess whether the head loss process has indeed changed after the addition of aluminum.

## 4. Control Charts for NEI Fiber Bed Data and Discussion

For each of the three CHLE head loss columns with the NEI fiber bed, we present the control chart with $\alpha$ = 0.05, both with the initial training period included and only after aluminum addition. For the NEI fiber beds, based on a preliminary analysis, it appeared that there may be responses at two points in time after aluminum was added. Thus, we consider a second training period starting at day 10.5 and ending at day 11.5, and we set new control limits for the process after that point. We also give the estimated $\lambda_1$ and $\lambda_2$ values for both training periods and the observation periods. Finally, we discuss the meaning of the charts for each column.

### 4.1 Column 1

***Period 1***

Training Fraction Outside Control Limits (two-sided) = 0.0694

Training Fraction Outside Upper Control Limit = 0.0417

Observed Fraction Outside Control Limits (two-sided) = 0.0953

Observed Fraction Outside Upper Control Limit = 0.0126

$\lambda_1 = 0.12$

$\lambda_2 = 0.43$

***Period 2***

Training Fraction Outside Control Limits (two-sided) = 0.0063

Training Fraction Outside Upper Control Limit = 0.0000

Observed Fraction Outside Control Limits (two-sided) = 0.0028

Observed Fraction Outside Upper Control Limit = 0.0021

$\lambda_1 = 0.07$

$\lambda_2 = 0.10$

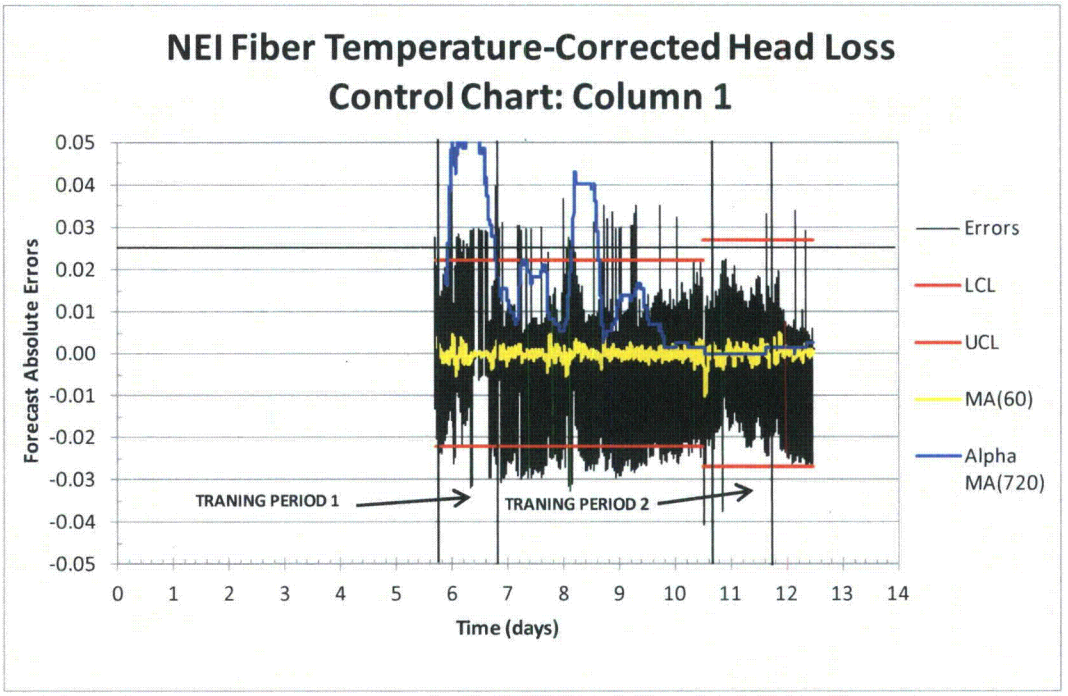


Figure 2. NEI Fiber Temperature-Corrected Head Loss Control Chart Column 1 - Initial Training Period Included. The figure depicts errors (see equation (1)), the lower control limit and the upper control limit (see equation (7)), a moving average of errors based on the last 60 one-minute periods, and a moving average of violations of the upper control limit for the last 720 one-minute periods. Subsequent figures have similar formatting.

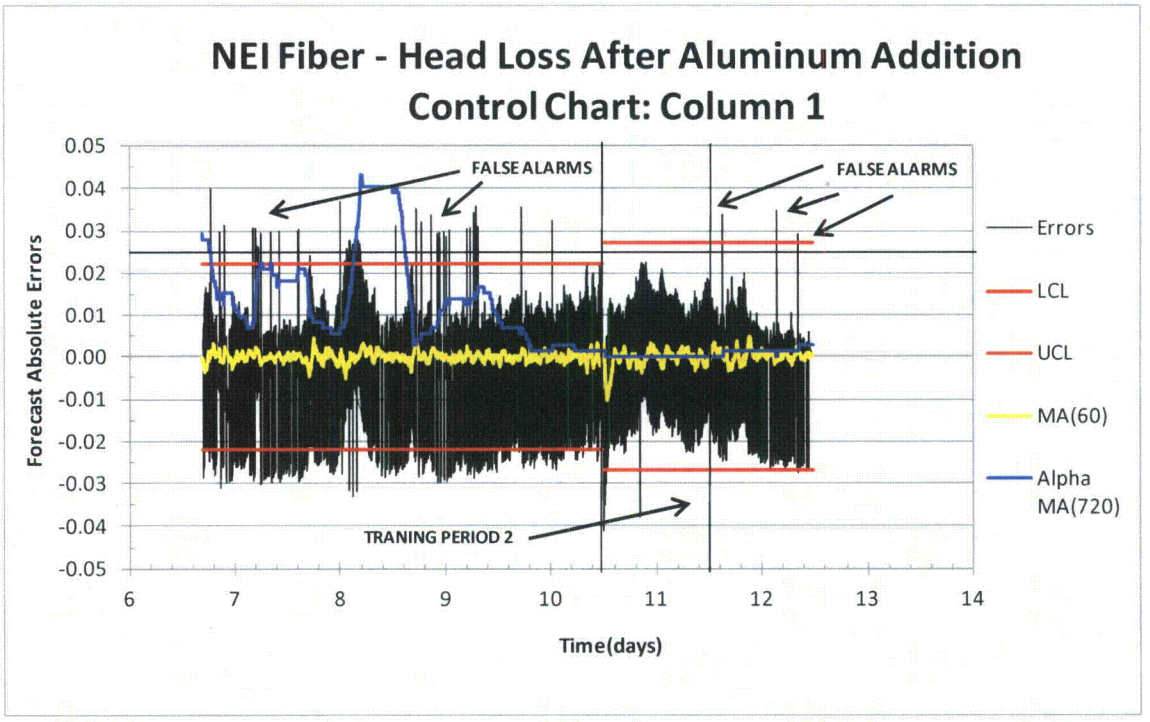


Figure 3. NEI Fiber Temperature-Corrected Head Loss Control Chart Column 1 - Initial Training Period Not Included

During the initial training period, the observed alpha value (i.e., the fraction of observations outside the two-sided control limits) of 0.0694 is slightly higher than the expected 0.05, but within reason, leading us to conclude the control limits are reasonable. During the initial observation period, the observed alpha value for two-sided violation rose to 0.0943. However, the fraction of violations of the upper control limit are only 0.0126, well within the expected value of 0.025. The only exception to this for a narrower time window is the denser mass of errors near the upper control limit depicted early in day 8; see Figure 2. The moving average of the rate of the upper control limit violation over half-a-day (720 minutes) grows to about 0.04, compared to an expected upper limit violation of 0.025, but we regard this as being at most a weak signal. An analogous analysis for the second period gives no indication of a signal. Based on this, we do not find compelling evidence that in column 1 there was a statistically significant increase in head loss as aluminum was added over time.

### 4.2 Column 2

***Period 1***

Training Fraction Outside Control Limits (two-sided) = 0.0958

Training Fraction Outside Upper Control Limit = 0.0243

Observed Fraction Outside Control Limits (two-sided) = 0.0892

Observed Fraction Outside Upper Control Limit = 0.0451

$\lambda_1 = 0.23$

$\lambda_2 = 0.00$

***Period 2***

Training Fraction Outside Control Limits (two-sided) = 0.0903

Training Fraction Outside Upper Control Limit = 0.0417

Observed Fraction Outside Control Limits (two-sided) = 0.1091

Observed Fraction Outside Upper Control Limit = 0.0539

$\lambda_1 = 0.15$

$\lambda_2 = 0.01$

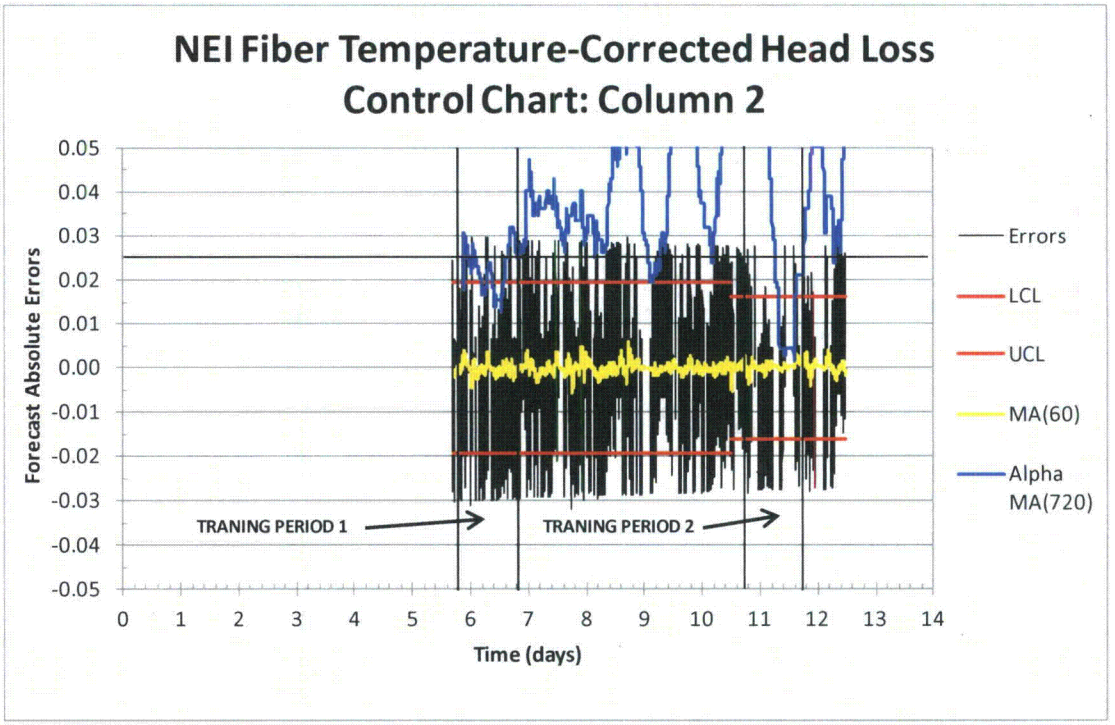


Figure 4. NEI Fiber Temperature-Corrected Head Loss Control Chart Column 2 - Initial Training Period Included

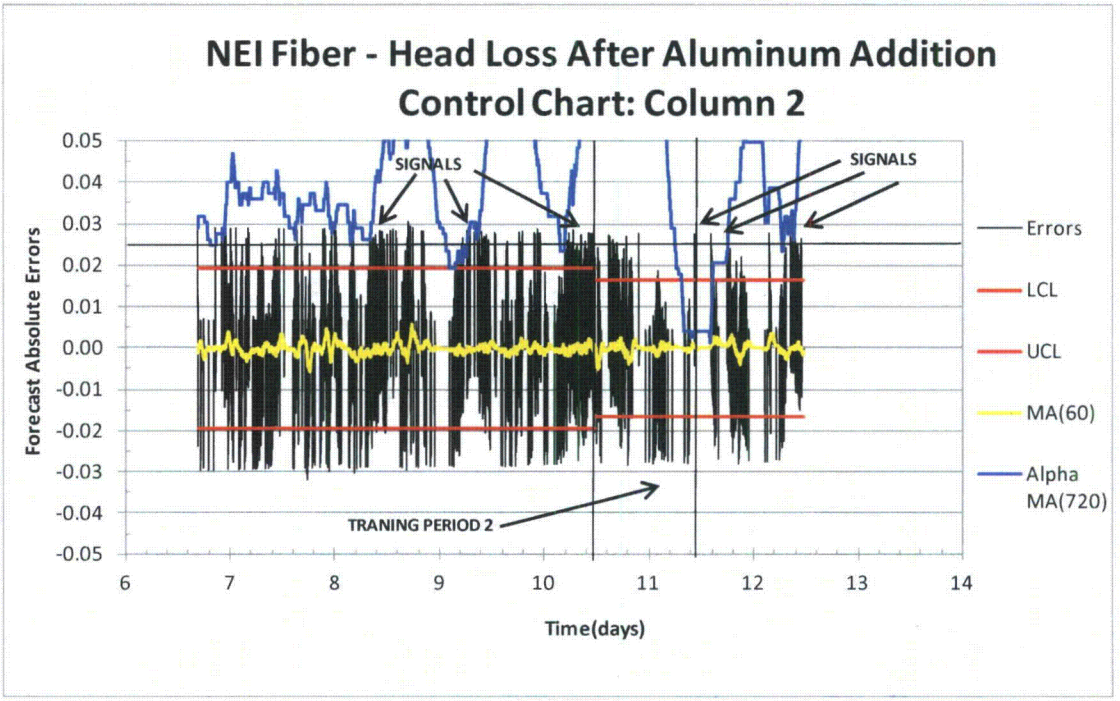


Figure 5. NEI Fiber Temperature-Corrected Head Loss Control Chart Column 2 - Initial Training Period Not Included

During the first training period, the observed alpha value of 0.0958 is again a bit higher than the expected 0.05, but perhaps close to within reason. The observed upper control limit violations of 0.0243 matches closely the expected 0.025 during the first training period. During the first observation period, the observed alpha value for upper control limit violations climbs to a modest value of 0.0451. However, as the moving-average values in Figure 4 depict, for substantial portions of day 8 and days 9-10.4, there are significant violations of the upper control limit. The associated "blue line" exceeds the chart's maximum, and peaks at 0.0625 during the first such interval (day 8) and 0.0722 during the second interval. There is similar behavior during the second period. So while the process is not consistently out of statistical control after the addition of aluminum, there are significant periods of more than one-half day in length where the process deviates well beyond the control limits. This suggests a statistically significant deviation of the process after the addition of aluminum. We further note that the timing of these deviations is consistent with visible jumps in the level of the head loss for column 2 in Figure 2 of Howe (2012).

### 4.3 Column 3

***Period 1***

Training Fraction Outside Control Limits (two-sided) = 0.0271

Training Fraction Outside Upper Control Limit = 0.0146

Observed Fraction Outside Control Limits (two-sided) = 0.0202

Observed Fraction Outside Upper Control Limit = 0.0130

$\lambda_1 = 0.11$

$\lambda_2 = 0.32$

***Period 2***

Training Fraction Outside Control Limits (two-sided) = 0.0125

Training Fraction Outside Upper Control Limit = 0.0097

Observed Fraction Outside Control Limits (two-sided) = 0.0135

Observed Fraction Outside Upper Control Limit = 0.0078

$\lambda_1 = 0.10$

$\lambda_2 = 0.13$

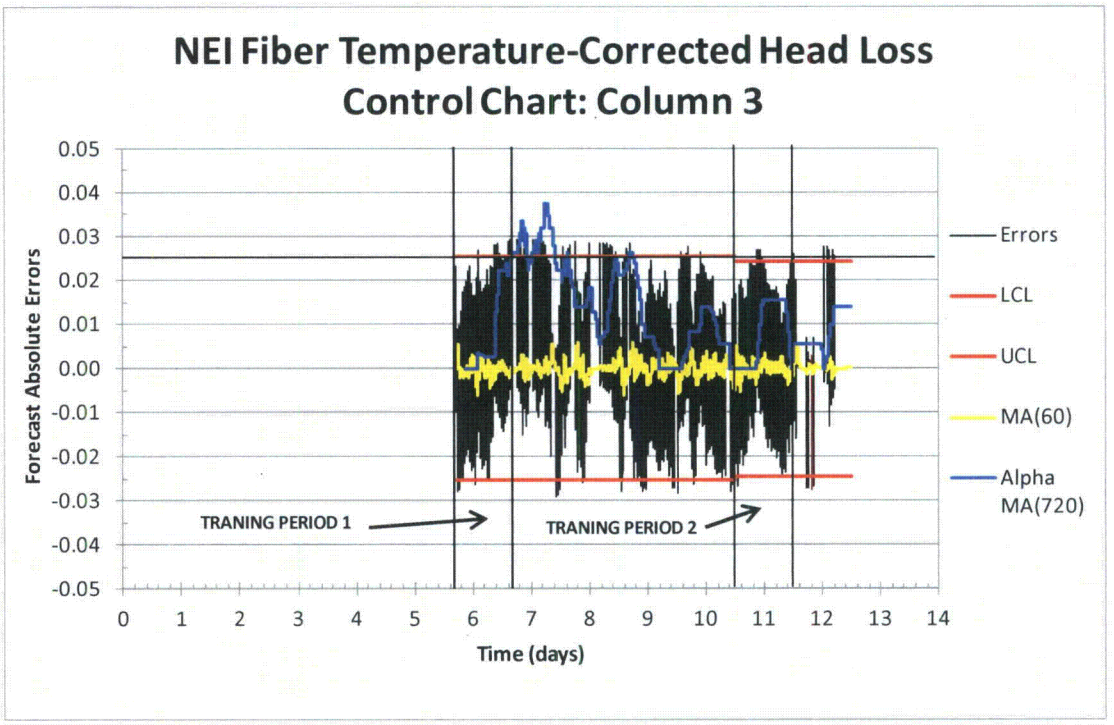


Figure 6. NEI Fiber Temperature-Corrected Head Loss Control Chart Column 3 - Initial Training Period Included

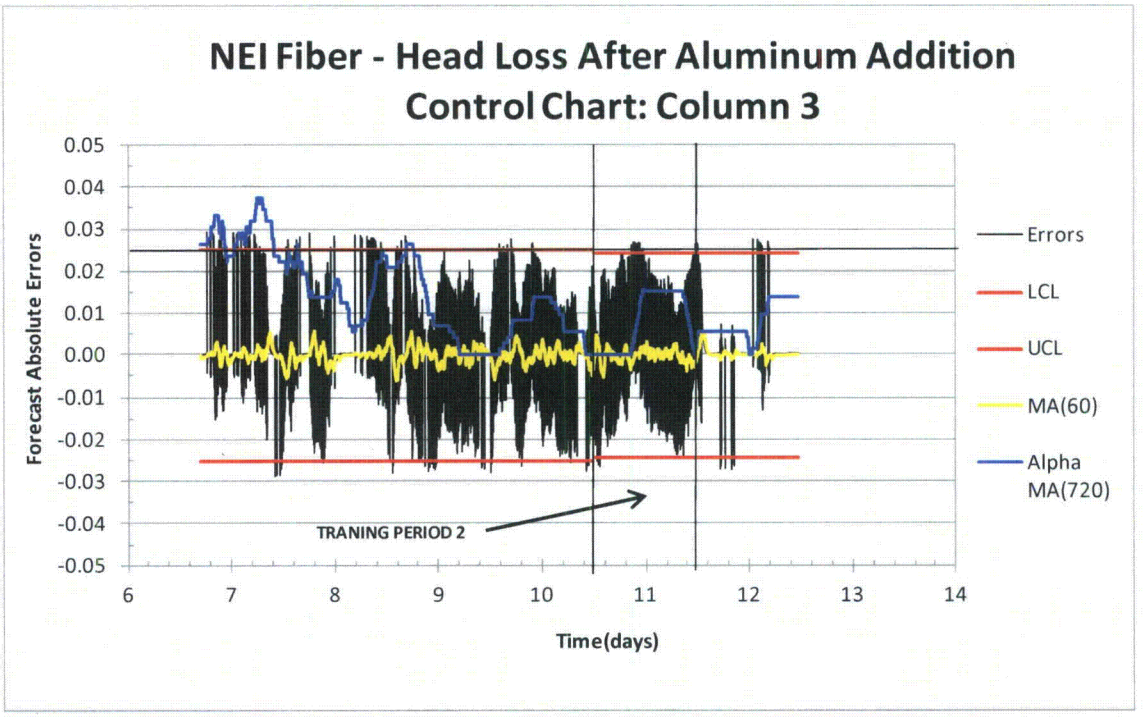


Figure 7. NEI Fiber Temperature-Corrected Head Loss Control Chart Column 3 - Initial Training Period Not Included

During both training periods and observation periods, the observed alpha values are less than 0.05 for violations of the two-sided control limits and less than 0.025 for violations of the upper control limit. Individual errors violate control limits only on rare occasions. The moving-average of violations of the upper control limit modestly exceeds 0.025 for part of day 7, but otherwise is almost exclusively below 0.025. It is reasonable to conclude that in column 3, there was not a statistically significant increase in head loss as aluminum was added over time.

**5. Control Charts for Blended Fiber Bed Data and Discussion**

Again for each of the three columns under the blended fiber bed data, we present control charts with $\alpha =$ 0.05 both with the initial training period included and only after the addition of aluminum. For the blended fiber beds, we only use one training period and one observation period. We again provide the observed alpha values and optimal smoothing parameters for both the training and observation period. The results here are not subtle for columns 1 and 2 and a formal statistical analysis is arguably overkill in these cases. (See Figure 1 of Howe, 2012.) We simplify the discussion slightly by not distinguishing two-

sided and upper-limit violations, and by suppressing presentation of the upper control limit violation, at least until the discussion in Section 5.3.

### 5.1 Column 1

Training Period Fraction Outside Control Limits = 0.0454

Observation Period Fraction Outside Control Limits = 0.3832

$\lambda_1 = 0.16$

$\lambda_2 = 0.48$

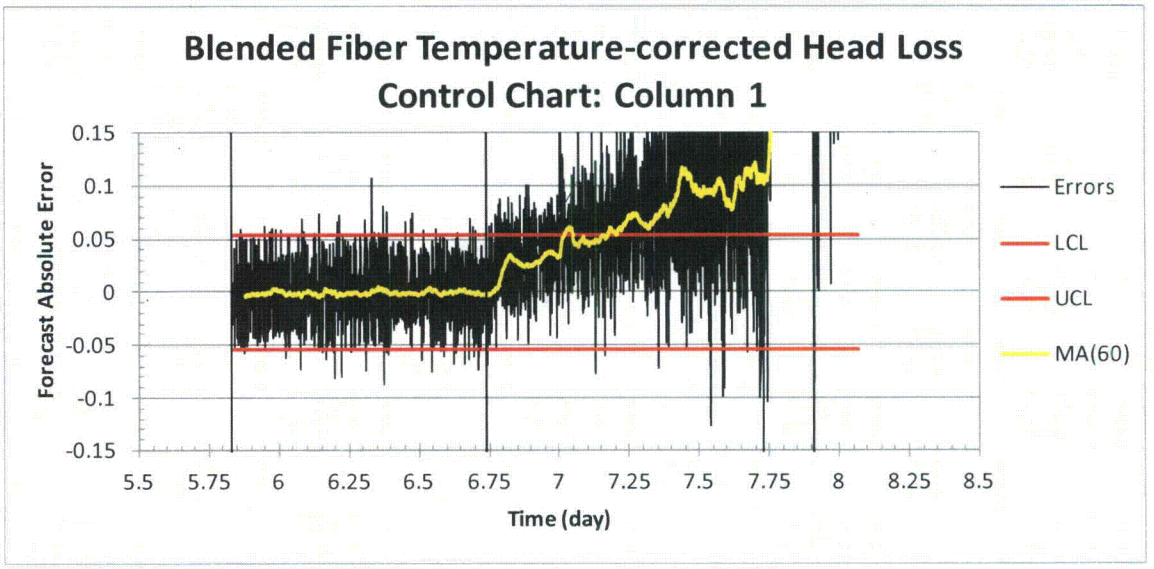


Figure 8. Blended Fiber Temperature-Corrected Head Loss Control Chart Column 1 - Initial Training Period Included

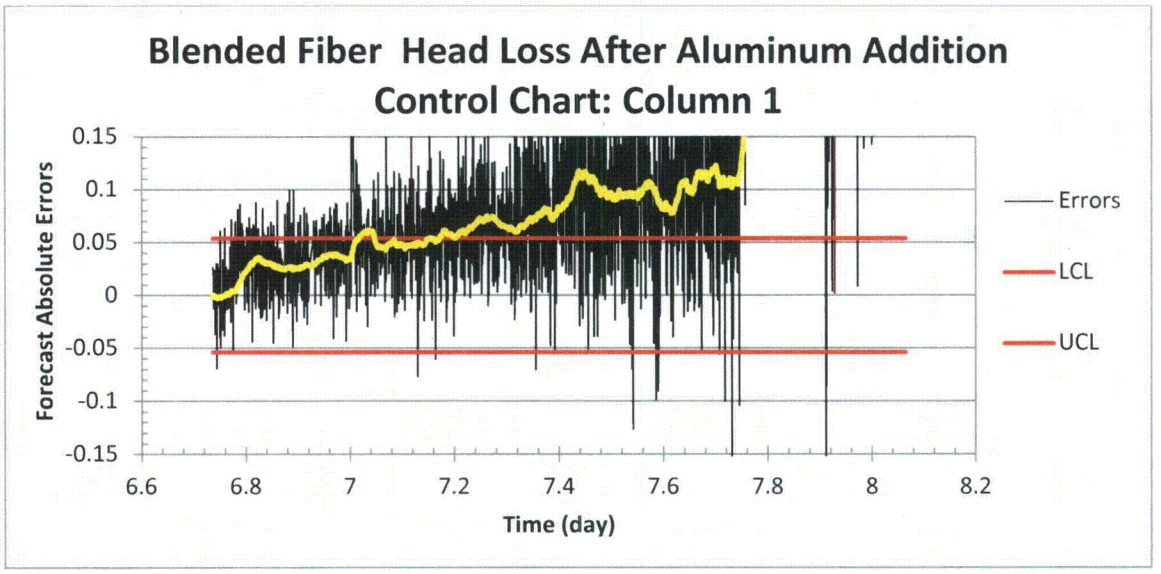


Figure 9. Blended Fiber Temperature-Corrected Head Loss Control Chart Column 1 - Initial Training Period Not Included

The observed alpha value during the training period of 0.045 is close to the expected 0.05, leading us to conclude the control limits set during training are sound. Examining Figure 7, the steady state assumption of the error process during the training period appears appropriate. From both Figures 7 and 8, we observe an almost immediate response after aluminum is added, with a delay of about 0.05 days. The one-hour moving average captures this change fairly well, and the errors quickly exceed the upper control limit. At about 7.3 days, the errors increase significantly and the process jumps to a further out-of-control state. In column 1, there is clearly a statistically significant response to the addition of aluminum, much more pronounced than with any of the NEI fiber beds.

### 5.2 Column 2

Training Period Fraction Outside Control Limits = 0.0477

Observation Period Fraction Outside Control Limits = 0.2462

$\lambda_1 = 0.40$

$\lambda_2 = 0.00$

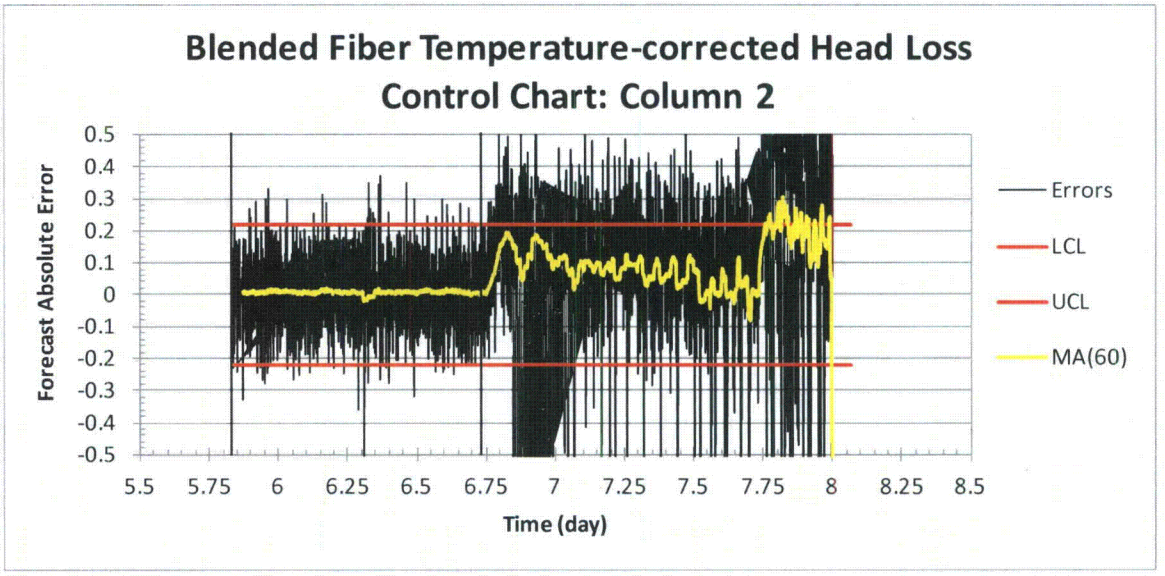


Figure 10. Blended Fiber Temperature-Corrected Head Loss Control Chart Column 2 - Initial Training Period Included

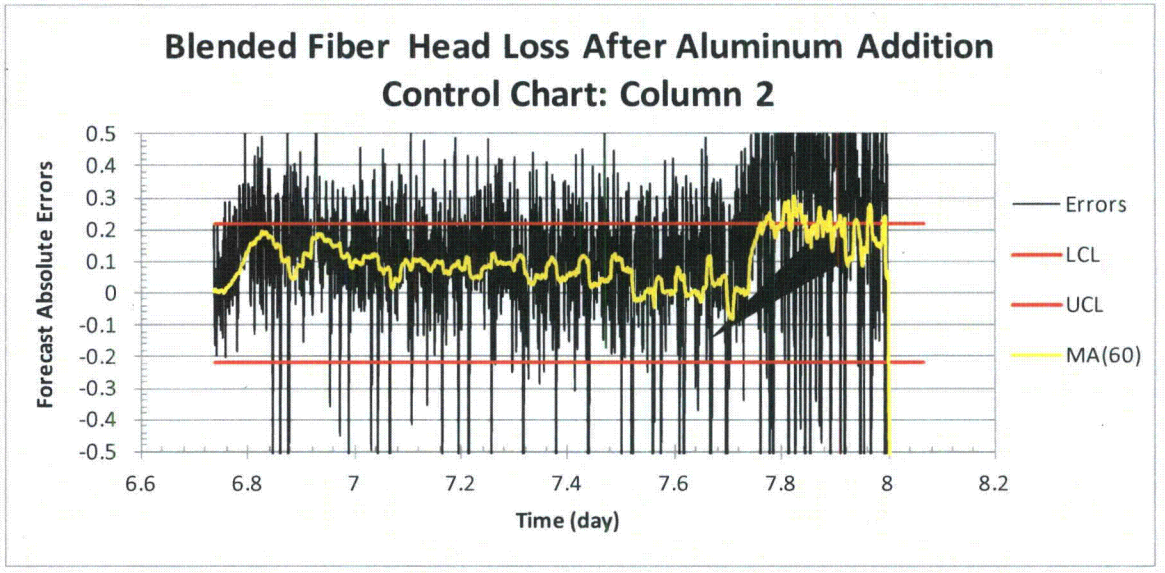


Figure 11. Blended Fiber Temperature-Corrected Head Loss Control Chart Column 2 - Initial Training Period Not Included

The observed forecast errors for column 2 are very similar to those of column 1. The observed alpha value during the training period is 0.045. From Figure 9, we see that the error process during the training period is relatively stable, consistent with a steady state error process. Examining Figure 10, we see

another immediate response after aluminum is added, with a delay of about 0.05 days. The one-hour moving average again captures this change fairly well and the errors quickly exceed the upper control limit. For this column, the error process appears to stabilize over the next day, and then at day 7.7 another large shift above the upper control limit occurs. In column 2, there is clearly a statistically significant response to the addition of aluminum.

### 5.3 Column 3

Training Period Fraction Outside Control Limits = 0.0293

Observation Period Fraction Outside Control Limits = 0.0525

$\lambda_1 = 0.60$

$\lambda_2 = 0.19$

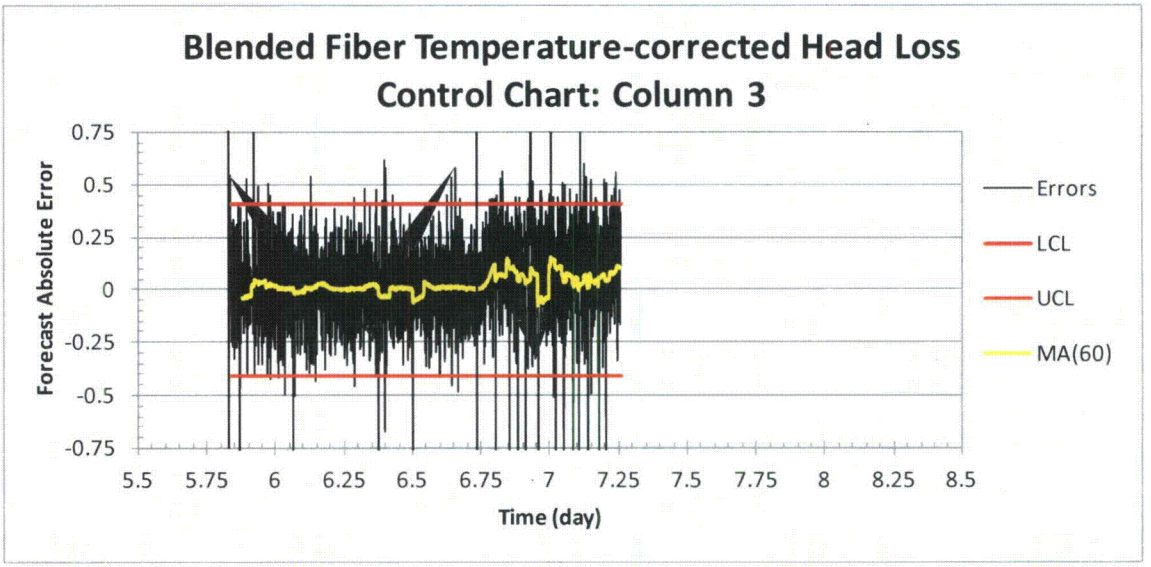


Figure 12. Blended Fiber Temperature-Corrected Head Loss Control Chart Column 3 - Initial Training Period Included

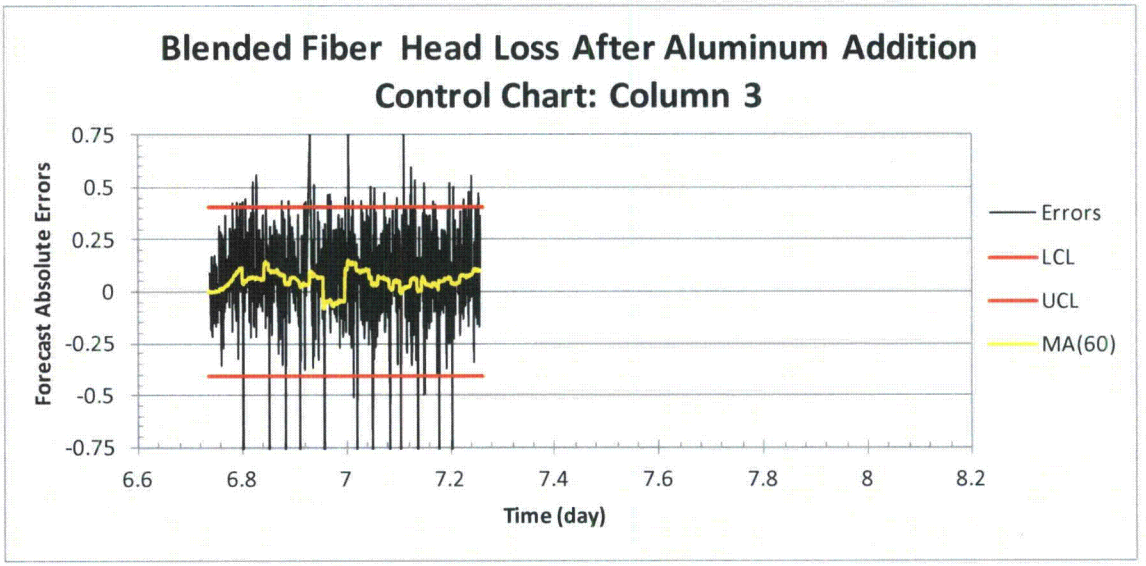


Figure 13. Blended Fiber Temperature-Corrected Head Loss Control Chart Column 3 - Initial Training Period Not Included

Examining Figure 1 in Howe (2012) for column 3, we see an apparent change in the process, i.e., an apparent change in slope. However, compared to columns 1 and 2 for the blended fiber beds, the volatility of column 3's process makes this more difficult to establish statistically. In contrast to columns 1 and 2, the observed violation of the two-sided control limits for column 3 is 0.0525. The fraction of violation of the upper control limit is 0.0324. However, when forming a moving average of the upper control limit violation of 720 minutes (not depicted in the figures) we find that the violation steadily climbs from around 0.014 at day 6.33 to 0.064 at day 7.25; i.e., the moving average climbs to a value substantially larger than the expected value of 0.025. While more subtle than columns 1 and 2, this suggests a change in the head loss process after the addition of aluminum. That said, the change is only statistically significant—according to the moving average measure—substantially later than for columns 1 and 2.

**References**

Croux, C., Gelper, S., & Mahieu, K. (2010 1-April). *Robust Control Charts for Time Series Data.* Retrieved 2012 5-August from http://dx.doi.org/10.2139/ssrn.1588646

Howe, K. (2012). *CHLE Tank Test Results for Blended and NEI Fiber Beds with Aluminum Addition.* University of New Mexico, Department of Civil Engineering, Albuquerque.